Aquaculture Reports 27 (2022) 101340

Contents lists available at ScienceDirect

Aquaculture Reports

journal homepage: www.elsevier.com/locate/aqrep

The parasitic travel of *Margaritifera margaritifera* in Atlantic salmon gills: from glochidium to post-larva

P.A. Castrillo [a], R. Bermúdez [a,b], C. Varela-Dopico [c,d], M.I. Quiroga [a,b], P. Ondina [c,d,*]

[a] Department of Anatomy, Animal Production and Veterinary Clinical Sciences, Faculty of Veterinary, Universidade de Santiago de Compostela, Lugo, Spain
[b] Instituto de Acuicultura, Universidade de Santiago de Compostela, Santiago de Compostela, Spain
[c] Department of Zoology, Genetics and Physical Anthropology, Faculty of Veterinary, Universidade de Santiago de Compostela, Lugo, Spain
[d] Instituto de Biodiversidade Agraria e Desenvolvemento Rural, Universidade de Santiago de Compostela, Lugo, Spain

ARTICLE INFO

Keywords:
Freshwater Pearl Mussel
Larval development
Glochidium
Mushroom body
Byssal gland

ABSTRACT

The larval development of the endangered freshwater mussel *Margaritifera margaritifera* (L.) represents one of the most unique parasitism among naiads, in which larva parasite the fish gills for several months. Despite the importance of this parasitic phase to successfully culture the freshwater mussel, the larval morphogenesis remains understudied. To describe the parasitic larval development and metamorphosis, Atlantic salmon (*Salmo salar* L.) were exposed to glochidia, sampled periodically to visualize the gills by stereomicroscopy and light microscopy and results were summarized throughout three developmental stages. Once attached to the fish gills, glochidia changed their morphology within the first days and acquired an intermediate stage termed mushroom larva due to the presence of the mushroom body and the zip membrane, both structures are transitory and distinctive of this long-lasting parasitism. The zip membrane, located at the valve cleft, may play a unique role in the isolation and acquisition of non-particulate nutrients from the fish, while the mushroom body of the mantle accumulates abundant intracytoplasmic lipid droplets. After 200 days, a successful metamorphosis was evidenced by the formation of a complete set of post-larval organs, pointing to the acquisition of different functionality, which will be essential for the settlement and deposit-feeding into the riverbed. Among the post-larval organs, the byssal complex of the post-larval foot was described for the first time at the end of the parasitic stage of naiads. In conclusion, this study provides an overview of the larval morphogenesis of *M. margaritifera*, from glochidium to post-larva, essential for understanding the parasitic interaction between the freshwater mussel larva and the fish host. Moreover, the morphological techniques and the hallmarks described might be applicable to optimize and monitor the larval developmental status during one of the most critical stages of the captive breeding programmes of endangered freshwater mussels.

1. Introduction

Freshwater mussels of the order Unionida are known as naiads, according to the mythological female nature deities which preside over bodies of fresh water and protect the water quality and the freshwater ecosystem. Naiads provide a direct contribution to human and animal health which depend on these resources (Strayer, 2017; Vaughn, 2018). These ecosystem services are expected to occur in large mussel communities, where the semi-infaunal adults display important burrowing and biofiltration functions in the riverbeds (Boeker et al., 2016; Vaughn and Hakenkamp, 2001; Vaughn et al., 2008). Nevertheless, freshwater mussels in the Northern Hemisphere are one of the largest and most threatened freshwater taxa worldwide (Lopes-Lima et al., 2018, 2017a). In Europe, *Margaritifera margaritifera* (Linnaeus, 1758) is listed as critically endangered (Lopes-Lima et al., 2018, 2017b), and most of the populations lack recent recruitment due to the loss of the habitat required by the young mussels (Geist and Auerswald, 2007).

Before the juvenile stage, the *M. margaritifera* embryo is brooded within the marsupia of parent mussels and develops into glochidium. This unique larval stage is released into the water to encyst into the gill epithelia of their salmonid host, *Salmo salar* L. and *Salmo trutta* L. fry and parr (Kat, 1984; Wächtler et al., 2001). After several months larva completes its metamorphosis and detaches from the host gills when temperature increases (Hruska, 1992). This embryological and larval

* Corresponding author at: Department of Zoology, Genetics and Physical Anthropology, Faculty of Veterinary, Universidade de Santiago de Compostela, Lugo, Spain.
E-mail address: mapaz.ondina@usc.es (P. Ondina).

https://doi.org/10.1016/j.aqrep.2022.101340
Received 30 November 2021; Received in revised form 16 September 2022; Accepted 16 September 2022
Available online 20 September 2022

development is regarded as a parasitic strategy for upstream dispersal and nutrition (Barnhart et al., 2008; Denic et al., 2015; Schwartz and Dimock, 2001), and contrasts with the pelagic veliger larva of other bivalves (Bändel, 1988; Carriker, 2001). Moreover, this interaction between the larva and the fish supposes an important parasitism among unionoideans, where the small glochidium of *M. margartifera* grows five folds from the initial size (Bauer, 1994; Denic et al., 2015; Howard and Anson, 1922; Scharsack, 1994; Scheder et al., 2011). Therefore, one of the eventual emergency conservation strategies relies on the captive culturing of the young mussels, in which the larva needs to successfully develop during this long-lasting parasitic larval stage on its suitable fish hosts (Gum et al., 2011).

Despite the importance of this parasitic phase for the subsequent survival of the juvenile mussels, very few studies focused on the anatomy of freshwater mussel adults (McElwain and Bullard, 2014). For instance, this parasitic stage has been characterized in other naiads such as the margaritiferid *Pseudunio auricularius* during its parasitism in Siberian sturgeon (*Acipenser baerii*) (Araujo et al., 2002). Moreover, other species as *Hyriopsis bialatus* and *Utterbackia imbecillis* develop large glochidium with brief parasitic stages on the fish, thus, a supplemented tissue culture with fish serum could be successfully employed to describe the short in vitro development of these larvae (Chumnanpuen et al., 2011; Fisher and Dimock, 2002). Recent studies described the morphology of free-living young *M. margaritifera* after metamorphosis and detachment from the gills, termed post-larval or juvenile stages (Araujo et al., 2018; Lavictoire et al., 2018; Schartum et al., 2016). However, up to our knowledge, there is only one study focused on the larval development of the threatened species *M. margaritifera*, by Scharsack (1994) in brown trout.

Based on these previous descriptions of the larval development, our hypothesis is that the parasitic larvae of *M. margaritifera* might acquire exclusive anatomical structures involved in the survival and development from glochidium to free-living freswater juveniles. In order to provide insight into the unique parasitic interaction between the *M. margaritifera* naiad and one of their hosts (*S. salar*), this study aims to thoroughly describe the larval development of the parasitic larva *M. margaritifera* in the salmon gills by stereomicroscopy and light microscopy. This knowledge will contribute to a better understanding of the pathogenesis of this parasitism as well as to improve the management of parasitic and post-parasitic larvae during the freshwater mussel conservation programmes.

2. Material and methods

Three independent experimental trials were performed from 2015 to 2018. Atlantic salmon fry (*S. salar*), coming from wild progenitors of the Ulla and Eo rivers, were artificially infested with glochidia and sampled periodically for approximately seven months to evaluate the microscopical morphology of the encysted larva. These experimental trials were carried out in the framework of a conservation aquaculture program, held in Lugo (Galicia, NW of the Iberian Peninsula) and focused on the propagation and captive breeding of this endangered freshwater mussel.

2.1. In vivo procedures in the salmon host

At the end of summer, salmon fry (age 0 +) were submitted to a glochidial exposure (Procedure 1) following the methodology described by Castrillo et al. (2020) (Fig. 1a and b). Briefly, wild gravid mussels of *M. margaritifera* (n = 2–4) were induced at each trial to oxygen and temperature stress to release and collect the glochidial spat. The released glochidia were evaluated in quantity and quality by light microscopy (number of viable larvae per millilitre). Thereafter, fry were exposed by bath immersion to 1000 glochidia g^{-1} of fish for 30 min, and subsequently reared in open system tanks of 0.5 m^3 and a density below 1.1 fish/L.

(a)

	trial	2015-16	2016-17	2017-18	mean
Glochidial exposure of fish (1)	date	01/10/2015	22/09/2016	24/09/2017	-
	fish (n)	1000	1000	500	-
Selection of infested fish (2)	days PE	202	177	169	182
	degree-days	2110	1633	1560	1752
	prevalence	8%	18%	35%	17%
Start of the detachment of viable post-larva (3)	days PE	209	194	190	198
	degree-days	2202	1809	1907	1996

(b) Fluctuations of water temperature in relation with the in vivo procedures

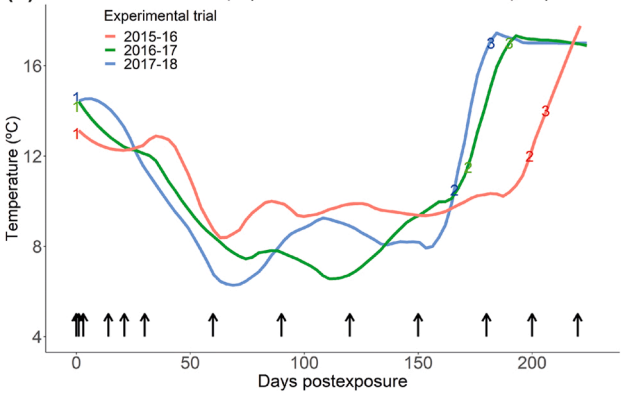

Fig. 1. Summary of experimental trials performed in Atlantic salmon fry during the 2015–16, 2016–17 and 2017–18, divided in three procedures. (a) Summarizing table of the different yearly procedures. (b) Fluctuations of the smoothed daily water temperatures through each trial (represented by different colours) in relation to the different procedures (1−3) and the 13 samplings (arrows).

Although a number of fish prematurely rejected the encysted larva, fish that remained infested after six months contained large larva encysted in the gill tissue, visible macroscopically by manual immobilization and abduction of the opercula (Castrillo et al., 2021). This technique allowed us to the in vivo diagnosis and selection of the infested fish (Procedure 2) showing a variable prevalence from 8% and 35% (Fig. 1a and b). Thereafter, infested fish (n = 40–78) were introduced in a recirculating system to synchronize the post-larval detachment (Procedure 3) by progressively increasing the water temperature up to 17 °C (Fig. 1a and b). Detached post-larva, also known as juveniles, were collected daily from the tank outlet by sieves and the start of the detachment of viable post-larva was determined at each trialwhen the majority of the detached individuals were viable (Fig. 1a).

To reflect the temperature fluctuations throughout each trial, the water temperature was monitored every three hours with a temperature data logger (UX100, Onset HOBO®), represented in relation to each experimental procedure (Fig. 1b). Moreover, to consider these different temperatures among trials, the elapsed accumulated temperature was calculated with the maximal and minimal values, expressed as the sum of the average daily water temperature in degree-days (Fig. 1a).

2.2. Sampling procedure

Based on the proportion of infested fish in the tank, from 6 to 10 exposed fish were sampled randomly at: 40 min and 1, 3, 14, 21, 30, 60, 90, 120, 150, 180, 200 and 220 days postexposure (PE; Fig. 1b). Each fish was anesthetized with an overdose of Tricaine methane-sulfonate (MS-222, Sigma-Aldrich®) and a bicarbonate solution (1:2); and the euthanasia was confirmed by sectioning cranially the spinal cord. Holobranches were excised and left gills were observed and photographed under a M125C stereomicroscope and a DM750 light microscope (Leica®). Additional squashes of small portions of the gill tissue without

the supporting arch were visualized directly by light microscopy. Larvae morphologically oriented in a lateral view were photographed with the light microscope objective at 10x (n = 5) to measure the larval shell length in the antero-posterior axis by ImageJ (Rueden et al., 2017).

Once the detachment from the fish gill was initiated, viable and unviable post-larvae were classified based on the presence or absence of pedal and valve movements, respectively, and photographed under the stereomicroscope to measure their length as previously described ($n = 40$, $\pm$ 0.1 μm). For the histological analysis of the detached post-larva, only the viable individuals were sampled to avoid potential post-mortem changes.

All procedures were carried out at the facilities of "Centro Ictiogénico de O Veral" (Xunta de Galicia) and followed the international (Directive 2010/63/EU, on the protection of animals used for scientific purposes), national (Law 6/2013 and RD 53/2013, on the protection of animals used for scientific experiments) and institutional regulations (USC Review Board).

2.3. Histology

Quickly after euthanasia, right holobranchs were fixed in Bouin's, Dietrich's and Davidson's fluids to compare the effect of the different fixatives and minimize the shrinkage artifacts of larvae due to potentially high osmolarity (Castrillo et al., 2020). After fixation for 18 h, right holobranchs were decalcified for 6 hr in a 10% ethylenediaminetetraacetic acid solution (Osteodec, Bio-optica®) and processed for histopathology by routine methods. Sections were stained with hematoxylin and eosin (H&E) and additional periodic acid-Schiff (PAS), PAS-diastase, PAS-alcian blue (PAS-AB) and Masson-Goldner trichrome stains were performed. During the most representative samplings of the last trial, left holobranches were fixed in 10% buffered formalin without the decalcification and stained with the calcium-specific stain alizarin red S; or sampled for cryosectioning and staining with H&E or the lipid-specific stain Sudan black B.

On the other hand, the sampled juveniles were fixed in Davidson's fluid for 3 h, rinsed in 10% ethanol, stained with a light solution of eosin, wrapped in a lens paper inside the cassettes and embedded by pipetting them, before being dehydrated and processed as aforementioned.

All slides were observed and photographed using a BX51 light microscopy equipped with an EP50 digital camera and a polarized light (Olympus®).

2.4. Statistical analysis

To estimate the relationship between the larval length and the accumulated temperature, the Kendall-Theil nonparametric linear regression and Spearman's correlation coefficient were calculated since data did not accomplish with the normality assumptions. On the other hand, the length of detached juveniles was compared between viable and unviable mussel with the parametric Student's t-test for hypothesis testing. The significance level was 95% in all cases (p-value <0.05). All the numeric data were analyzed by RStudio software (Anon, 2019).

3. Results

During the encystment in the gills of Atlantic salmon, the parasitic larvae of *M. margaritifera* grew and displayed a progressive organogenesis which led to the metamorphosis and detachment of the viable post-larva. To summarize the larval development during this long-lasting parasitism, the descriptions of each sampling point were grouped in three parasitic stages (I–III), based on the main morphological changes

Table 1
Summary of the main morphological changes observed during the parasitic development of *M. margaritifera* larvae encysted in the Atlantic salmon gills, grouped in three parasitic stages (I–III) represented each with a tranversal histological section.

Developmental stages	(I)	(II)	(III)
	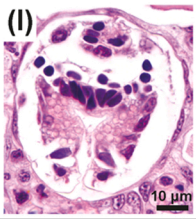	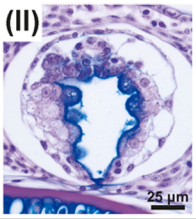	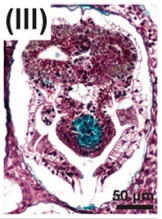
days postexposure (PE)	0-3	14-150	150-220
degree-days	0-37	130-1400	1400-2500
min-max length (μm)	60-72	72-293	308-397
external morphology	walnut shape semi-transparent	roundish-bean shape semi-transparent	bean shape opaque
valve cleft	disintegrated fish gill tissue	zip membrane	zip membrane elongation
inner mantle epithelium	loss of coarse intracytoplasmic granules	mushroom body	mushroom body regression
digestive apparatus	absent	discontinuous and immature digestive tract	mature digestive tract and primordium of the digestive gland
foot	absent	absent	ciliated and glandular foot
gills	absent	absent	three ctenidia per side
musculature	atrophy of the larval adductor muscle	absent	adductor and pedal musculature
other systems	absent	apparition of haemolymphatic cells	renopericardial, haemolymphatic and sensory systems

summarized in Table 1.

3.1. Parasitic stage I

This short stage comprised the first three days of the parasitism, from 40 min PE to 3 days PE. From the day 0 to the day 1 PE, glochidia became encysted into the gill tissue and lost their typical morphology specialized for clasping to the fish mucosa (Table 1). Initially, glochidia were completely encircled by the gill tissue and showed a walnut shape, approximately 60 μm length and 70 μm height (Fig. 2a). By histology, larvae were pinched to the gills by contraction of the larval adductor muscle clasping a small portion of host epithelium inside the pallial cavity. This pinched tissue became rapidly disintegrated in contact with the internal mantle epithelium, the latter characterized by the presence of eosinophilic, PAS positive and coarse intracytoplasmic granules (Fig. 2b and c). Exceptionally, very few glochidia failed to encyst at day 1 PE, observed with the valves wide open inside the gill tissue (Inset, Fig. 2a). At day 3 PE, larvae showed a negligible growth and the glochidial appearance was completely lost, confirmed by the absence of the clasped gill tissue, atrophy of the adductor muscle and loss of the granular appearance of the inner mantle (Fig. 2d).

3.2. Parasitic stage II

This stage, comprised from the day 14 to the day 150 PE (around the degree-day 130 and 1400 PE), was characterized by a pronounced increase in length in most of the larvae (71.8 ± 3.2 up to 293 ± 2.4 μm), the formation of the zip membrane and the profuse development of the mantle, especially the mushroom body (Table 1).

In detail, larvae were externally characterized by the acquisition of bean-shaped valves, elongated in the antero-posterior axis since the degree-day 500 PE (Fig. 3a). Each valve was formed by a semi-transparent and single layer of thin and continuous periostracum (below 1 μm thick), in intimate contact with the surrounding host tissue (Fig. 3a and b). Exceptionally, at the center of the hinge, the larval ligament was observed uncovered by periostracum (Fig. 3c) and conformed internally by a basophilic U-shaped structure around 2 μm height (Fig. 3d). The remaining valve cleft observed between the valve rims in the gill squash (Fig. 3a), was filled by the zip membrane since the degree-day 260 PE, identified as a membranous structure that isolated the pallial cavity from the surrounding host medium (Fig. 3e–g). This membrane was composed of a homogeneous, acellular and basophilic material; stained magenta-blue under the PAS-AB stain (Fig. 3 f) and turquoise-green under the trichrome stain (Inset, Fig. 3 g). Initially, the zip membrane arose as a thin and narrow structure which progressively became wider, increasing in width since the thedegree-day 800 PE onwards (Fig. 3 g).

Due to the translucent valves, the larval mantle could be observed composed of an inner and outer epithelium with abundant refringent vacuoles clustered concentrically, evidenced by visualization of the gill squashes (Fig. 4a). The outer layer was composed of a simple squamous epithelium that progressively acquired a cuboidal morphology, with a peripherally located nucleus and a vacuolized cytoplasm with extensions towards the inner epithelium (Fig. 4a–f). The central zone of the inner epithelium was covered mostly by the mushroom body (Fig. 4b). This structure was composed of abundant, tightly packed and highly globose cells with their cytoplasm extended apically, acquiring the characteristic mushroom-like appearance (Fig. 4b). Both outer and inner epithelium contained abundant lipid droplets, intensely stained black-blue under the Sudan black B stain (Fig. 4c). In detail, each cell contained a round and extensive nucleus (7–8 μm of diameter) with a marked nucleolus and abundant vacuoles up to 2 μm diameter dispersed all over the basal region of the cytoplasm (Fig. 4d). Moreover, an abundant and finely granular intracytoplasmic material (blue-magenta under the PAS-AB, diastase-resistant and slightly green-blue under the trichrome stain) was observed at the mushroom body and being secreted towards the pallial cavity (Fig. 4e and f). The apical membrane of these

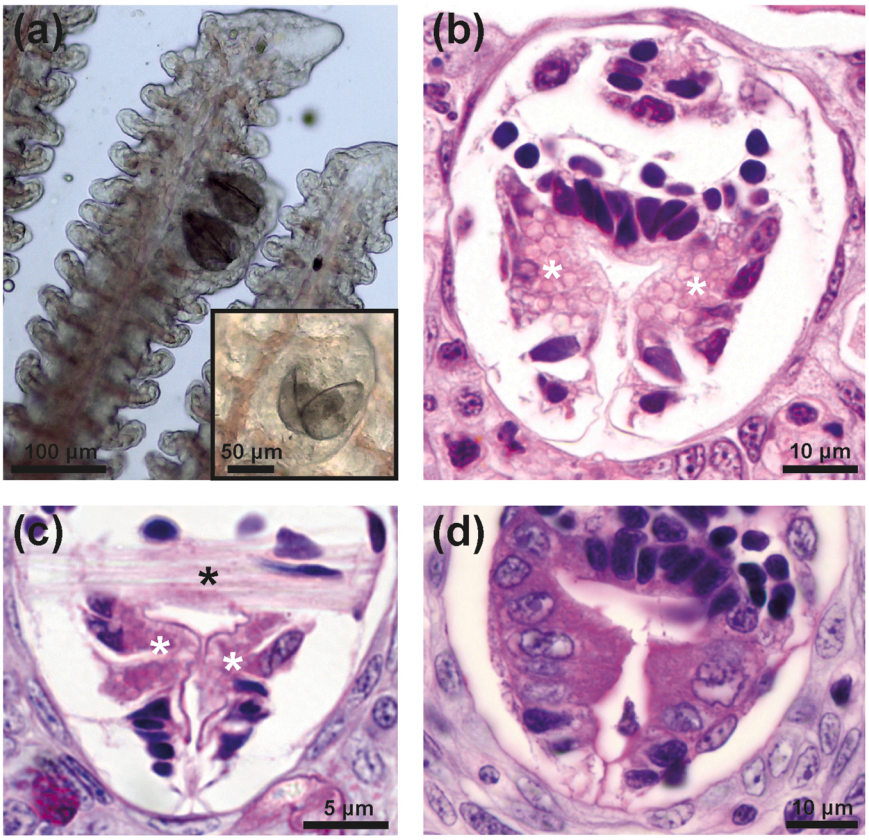

Fig. 2. Stage I of the parasitic larva of *M. margaritifera* encysted in the Atlantic salmon gills during the day 0–3 postexposure (PE). (a) Light microscopy of two recently encysted glochidia within the fresh gill tissue with closed valves and walnut shape. A few larvae failed to encyst, observed with their valves wide opened (Inset). (b–d) Histological sections of the closed bivalve, surrounded by the gill host tissue and showing at day 1 PE the inner mantle with coarse intracytoplasmic granules (white asterisks), eosinophilic (b) and PAS positive (c); becoming lost at day 3 PE (d). Anchored at both valves, the single larval adductor muscle (black asterisk, c) became atrophied and was absent at day 3 PE (d). H&E (b) and PAS stains (c and d).

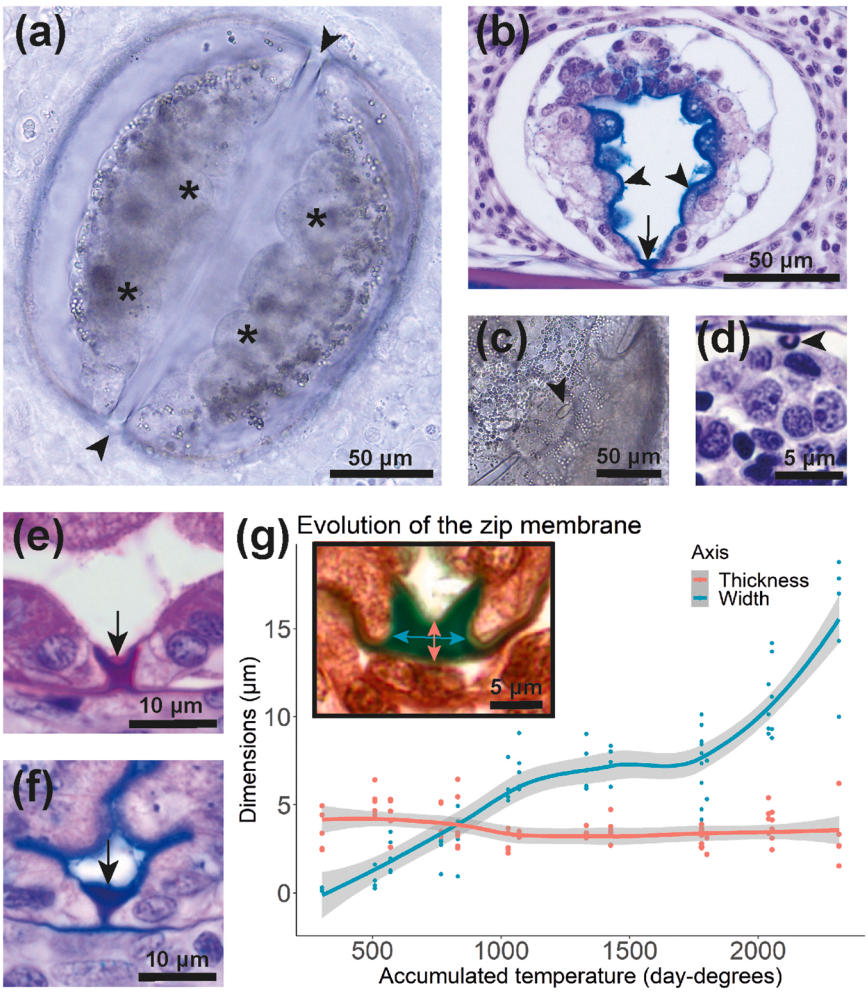

Fig. 3. Stage II of encysted larva of *M. margaritifera* from the day 14 to day 150 post-exposure (PE). (a) The gill squash of a bean-shaped larva highlights a pair of semi-transparent and continuous valves, the cleft between the valve rims (arrowheads) and the globose inner mantle cells (asterisks). (b) By light microscopy, the zip membrane (arrow) and the apical surface of the inner epithelium of the mantle was stained blue under the PAS-AB stain (arrowheads). (c and d) Microphotographs of the hinge region, located at the dorsal region, with a well-localized discontinuity on the periostracum (arrowhead, c), related to a basophilic U-shaped structure underneath under the H&E stain (arrowhead, d). (e and f) Comparison of a detailed histological section of the zip membrane (arrows) under PAS (e) and PAS-AB stain (f). (g) Evolution of the zip membrane dimensions (thickness and width) represented along the parasitic stages in the smoothed scatter plot. Inset: details of the zip membrane morphology highlighting the thickness as the distance among the periostracum of each valve (red arrow) and width as the distance among the external and outer surface of the zip membrane (blue arrow). Trichrome stain.

globose cells was lined with microvilli, forming a brush border epithelium (Fig. 4 f). At the marginal zone, the inner mantle epithelium between the mushroom body and the pallial edges was composed of basophilic cuboidal cells which progressively became more abundant at the end of this stage (Fig. 4d).

At the visceral mass of the larvae, abundant immature cells were observed with a small nucleus and basophilic cytoplasm. At the central region, a discontinuous digestive tract was progressively evidenced since the degree-day 300 PE as a cluster of cells concentrically arranged forming a small lumen around the degree-day 1000 PE (Fig. 4g). The epithelial cells shaping this tubular structure showed a simple and columnar epithelium, lacking cilia and with nucleus at basal position (Fig. 4g). Haemolymphatic cells were observed since the degree-day 1000 PE, with a PAS positive cytoplasm, loosely located at the dorso-posterior region without lining endothelium (Fig. 4h).

In contrast to this pronounced larval development, a few larvae showed a delayed development since the degree-day 300 to the degree-day 1000 PE, characterized on the gill squashes by the roundish shape, small size (approximately half the size of the bean-shaped larvae) and poorly discernible mantle structures (Fig. 4i).

Tissue fixation led to the occurrence of shrinkage artifacts that hindered the evaluation of the internal morphology of the larvae by histology, especially at the end of this stage. An inwards displacement of larval structures and tissues was observed in the most marked cases as hyperstained and irregular cell masses without discernible cell boundaries (Fig. 4j). By comparison of the different fixatives, Dietrich's fluid avoided the cell shrinkage causing minimal histological distortion, despite a moderate inward tissue displacement that remained present during all the study. On the other hand, the fresh frozen sections did not exhibit this artefactual displacement (Fig. 4k) and revealed an external empty cavity all over the outer surface of the zip membrane, well-delimited by flattened gill epithelial cells and completely isolated from the external medium (Fig. 4l and m).

3.3. Parasitic stage III

From the day 150 and 220 PE (around the degree-day 1400–2500 PE), the encysted larvae ranged from 308 ± 17–397 ± 27 µm length and suffered a metamorphosis, confirmed by the formation of most of the organs which constitute the plantigrade, or post-larva (Table 1). The morphological differences between the pre-metamorphosed and the encysted post-metamorphosed larva or post-larva, could be chronologically stablished before and after the day 200 PE or the degree-day 2000 PE, almost coincident with the mean start of the detachment of viable post-larva (Fig. 1a).

From the day 150 to the day 200 PE (the degree-day 1400–1800 PE), the pre-metamorphosed larva was characterized by a partially developed digestive tract, foot and gills. Valves progressively darkened in contrast with the previous stage, hindering the visualization of the internal morphology on the gill squashes (Fig. 5a). Regarding the mantle, the outer epithelial cells acquired a highly vacuolized cytoplasm with an intensely basophilic and PAS positive homogeneous material deposited as an amorphous thin layer over the inner side of the periostracum (Fig. 5b–d). On the other side of the mantle, the inner cuboidal epithelium occupied a wider mantle region than at the stage II and became as extensive as the mushroom body (Fig. 5b).

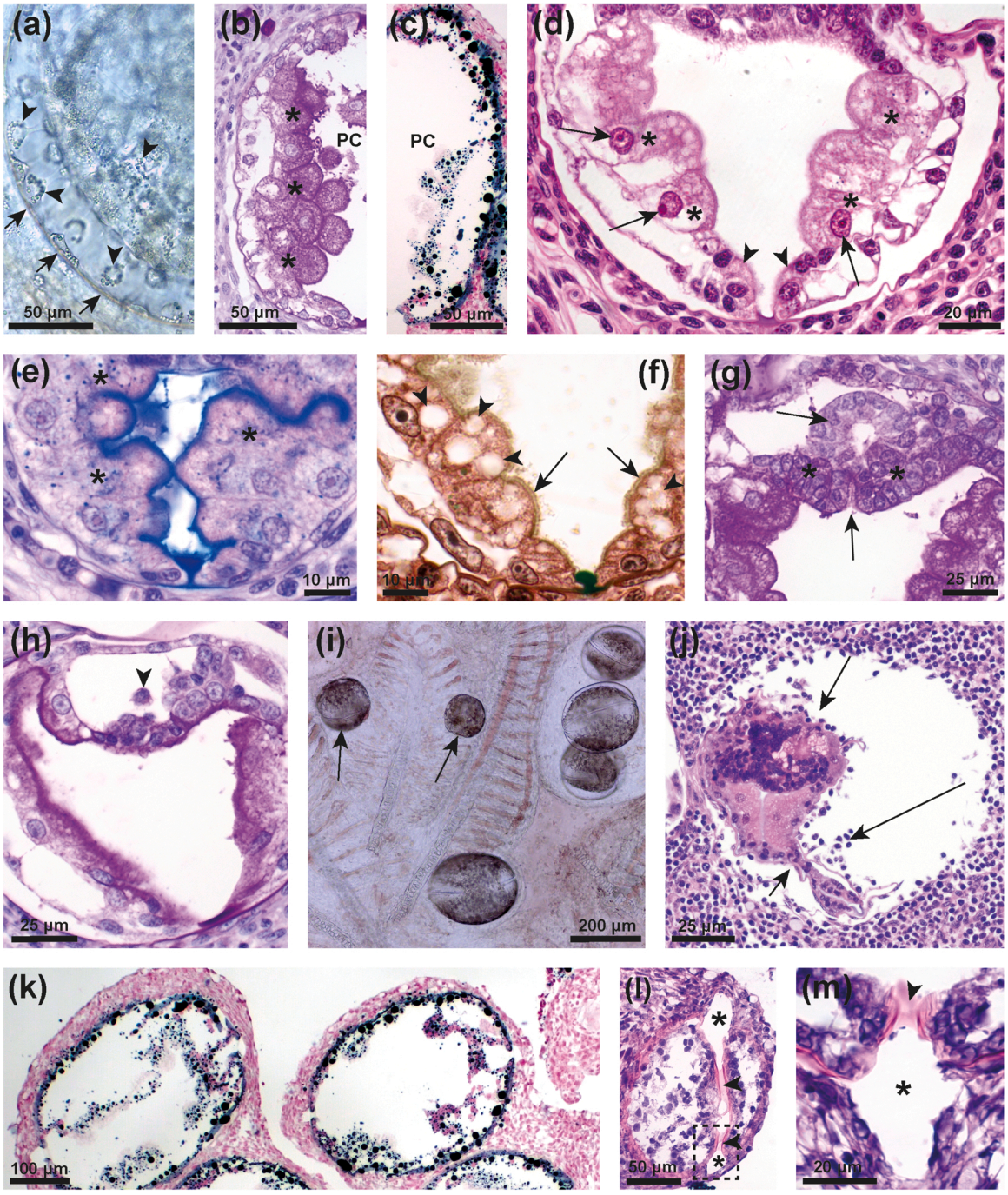

Fig. 4. Stage II of the encysted *M. margaritifera* larva from the day 14 to the day 150 post-exposure. (a) Gill squash showing highly vacuolized mantle cells (arrowheads) which lied over the thin periostracum of the valves (arrows). (b) Light microscopy of the larval mantle displaying the outer mantle cells and the characteristic mushroom body at the inner mantle (asterisks), composed by globose cells showing a vacuolized and PAS positive cytoplasm which protruded towards the pallial cavity (PC). PAS stain. (c) Specular view (in relation to b) of a dorsal histological section of the mantle highlighting in black-blue the lipid vacuoles located both at the larval mantle surround the pallial cavity (PC). Sudan black B stain. (d) The larval mantle was composed by an outer and inner epithelium, the latter composed by the extensive mushroom body oriented towards the center of the pallial cavity (asterisks) and basophilic cuboidal cells at the pallial edges (arrowheads). Note the globose cells of the mushroom body with a round nucleus (arrows) with an evident single nucleolus. H&E stain. (e-f) Detail of the mushroom body containing a PAS positive intracytoplasmic granular material (asterisks, e) and abundant vacuoles (arrowheads, f). Note the brush-border at the apical region (arrows, f). PAS and trichrome stains, respectively. (g and h) Visceral region of the larva showing abundant immature cells (asterisks, g), a discontinuous digestive tract (arrow, g) and a haemolymphatic cell (arrowhead, h). PAS stains. (i) Gill squash evidencing two small larva at the upper left corner (arrows), with a roundish shape and poorly identified mantle structures, in contrast with larger larva (right and lower side). (j) Inner displacement (in the direction of arrows) of the larval internal structures together with the surrounding gill tissue of the fish, due to histological artifact during tissue processing. (k) Fresh frozen section without histological shrinkage, also evidencing abundant lipid vacuoles highlighted in black-blue. Sudan black B stain. (l and m) Detail of the well-delimited external cavity (asteriks) over the zip membrane (arrowheads), only visible in the frozen sections. H&E stains.

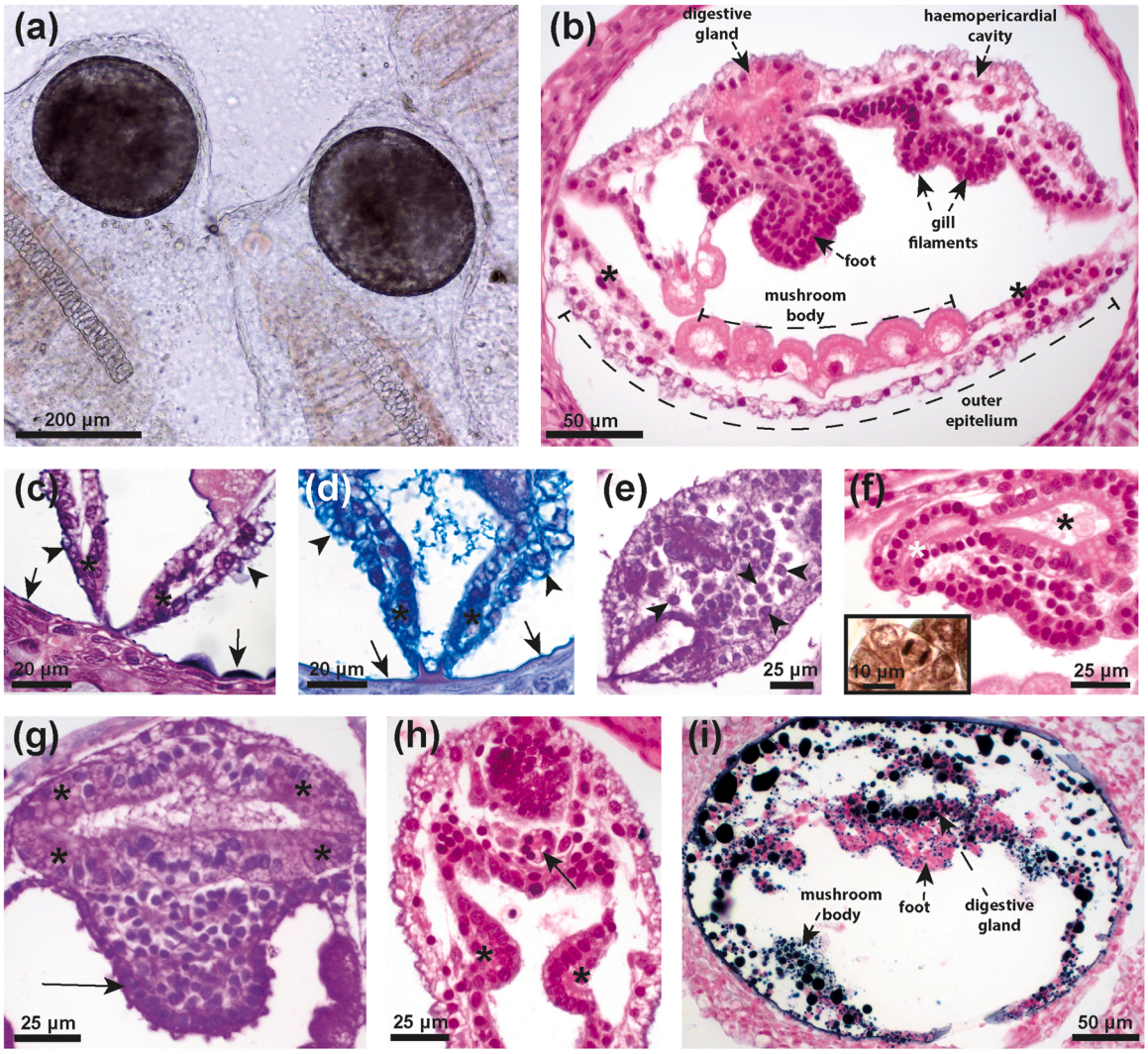

Fig. 5. Stage III of the *M. margaritifera* pre-metamorphosed larva encysted in the salmon gills from the day 150 to the day 200 post-exposure. (a) Squash showing a pair of larvae with partially opaque valves, encysted in two gill filaments. (b) Low magnification of a histological section of an encysted larva showing the partially developed foot, gill filaments, digestive gland and haemopericardial cavity. The extensive inner cuboidal epithelium (asterisks) and the mushroom body can be distinguished in the inner part of the mantle, as well as the outer epithelium located towards the valves. H&E stain. (c and d). Detail of the mantle margin (asterisks) showing the basophilic and PAS positive amorphous material over the outer mantle epithelium (arrowheads) and below the periostracum (arrows). H&E and PAS-AB stains, respectively. (e) Dorsoposterior region of the larva containing several haemolymphatic cells (arrowheads). PAS stain. (f). Anterior portion of the digestive tract showing a hyperplastic and poorly ciliated epithelium of the oesophagus (white asterisks) and stomach (black asterisk). H&E stain. Inset: Mitotic figure within the digestive lining epithelium. Trichrome stain. (g) Transversal histological section at the central region of the larva with the bilobed primordium of the digestive gland containing PAS positive granules (asterisks) as well as the primordium of the foot (arrow). PAS stain. (h) Transversal section at the posterior region of the larva where a pair of evaginated gill filaments (asterisks) and a portion of the intestine (arrow) were observed at the visceral mass. H&E stain (i) Frozen section showing abundant lipid vacuoles, highlighted black-blue all over the different larval tissues. Sudan black stain.

At the visceral mass, the formation of the different portions of the digestive tract was accompanied by the apparition of a low number of haemolymphatic cells at the dorsoposterior region (Fig. 5e). The digestive epithelium was hyperplastic and not completely differentiated, with poorly ciliated cells and abundant mitotic figures (Fig. 5 f and Inset). Moreover, since the degree-day 1600 PE, two bilateral evaginations arose antero-dorsally from the stomach, giving rise to a bilobed primordium of the digestive gland composed of highly granular epithelial cells (Fig. 5 g).

Towards the pallial cavity, the foot and the gills protruded ventrally and became hyperplastic showing an evaginated epithelium consisting of poorly organized and poorly differentiated cells with scant basophilic cytoplasm and abundant mitosis (Fig. 5b, g and h). The primordium of the foot arose from the central region of the visceral mass (Fig. 5 g); while the gill buds (between one and two) began to evaginate at both sides of the posterior region (Fig. 5 h). All organs were infiltrated by abundant lipid droplets of variable sizes as demonstrated with the Sudan black stain (Fig. 5i).

After metamorphosis, the post-larva was observed encysted in the gills between the day 200 and 220 PE (the degree-day 1900–2500 PE) and was characterized by the concurrence of post-larval organs/tissues (e.g. digestive tract, musculature, foot, ctenidia and nephridia; Fig. 6a–e) with the larval structures described during the stage II (mushroom body and zip membrane). Valves were mostly opaque and black-brown all over their surface except the anterior and posterior adductor muscle insertions that appeared as partially translucent and roundish areas on the valves (Fig. 6a). The valve clefts were completely occluded by the zip membrane (Fig. 7a–c), which was wider(Fig. 3 h) and intensely magenta stained under the PAS-AB when compared to previous stages. Moreover, the pallial edges folded inwards so an outer and inner fold became discernible (Fig. 7a–c). Each valve was composed by an outermost layer of continuous periostracum with homogeneous

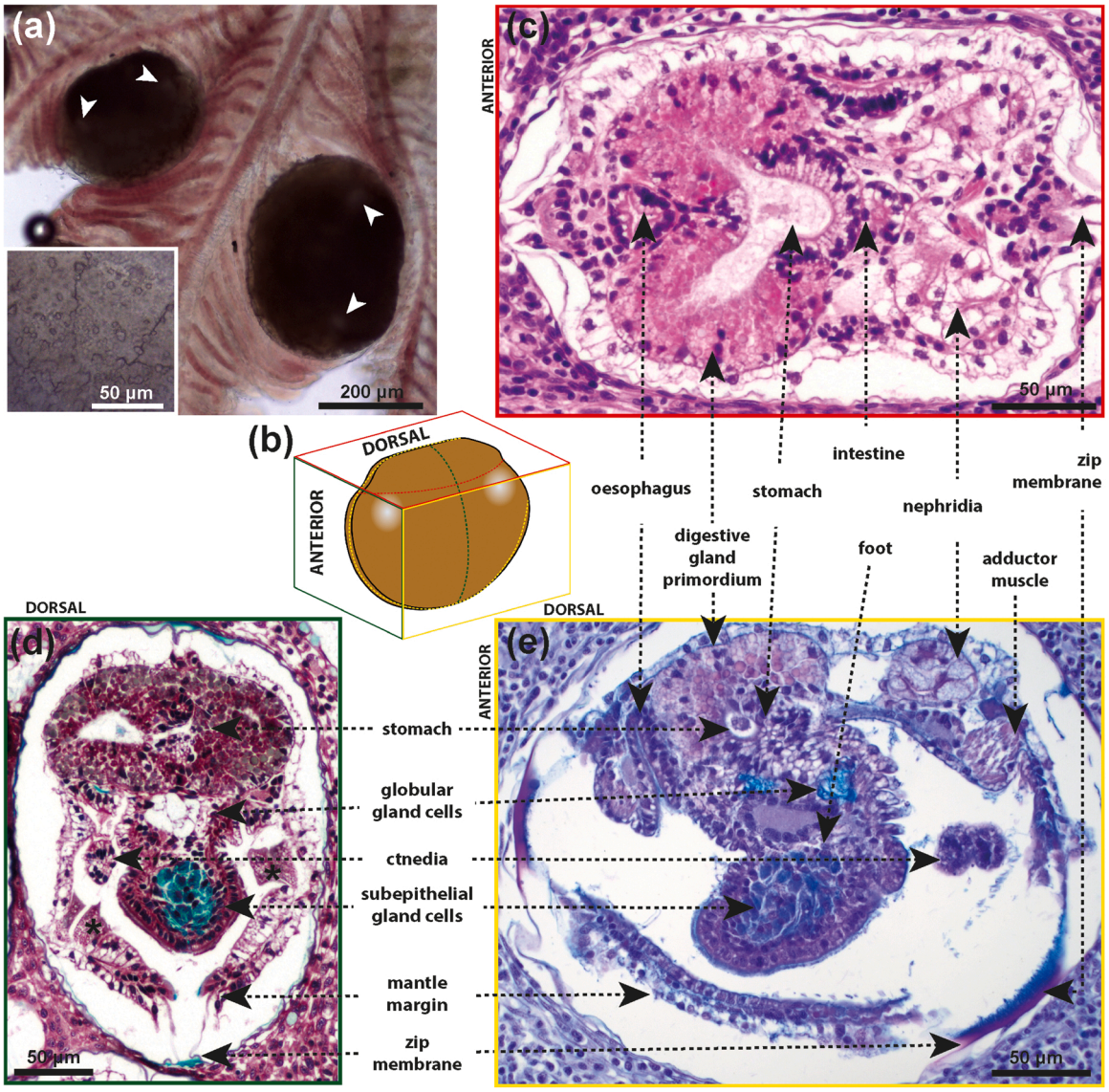

Fig. 6. Three-dimensional representation of the anatomy of the stage III of *M. margaritifera* post-larva encysted within the Atlantic salmon gills between the day 200 and 220 post-exposure. (a) Gill squash with two encysted post-larva showing almost entirely opaque valves, excepting the two insertions of the adductor muscles (white arrowheads). Inset: Higher magnification of the valve surface showing a black-brown colour. (b) Diagram of the post-larval shell, viewed from the left side, and showing the two adductor muscle insertions (white areas) in relation to three anatomical planes of section highlighted in red (dorsal), green (transversal) and yellow (longitudinal). (c-e) Representation of the main organs and structures in the different sections. (c) Dorsal histological section. H&E stain. (d) Transversal histological section. Trichrome stain. (e) Longitudinal histological section. PAS-AB stain.

thickness below 1 µm, birefringent under the polarized light (Fig. 7d). Moreover, a fibrous ligament with similar staining properties to the periostracum was evidenced underneath the U-shaped ligament, protruding inwards as a semioval structure with approximately 22 µm length and 11 µm height (Fig. 7e and f).

A thin basophilic layer coated irregularly the inner face of the periostracum (Fig. 7g). This material, stained blue by PAS-AB (Fig. 7h), did not stain specifically under the alizarin red S nor the trichrome stain (Fig. 7i). On the other side, the internal epithelium of the mantle resembled that of the adult mussel since the mushroom body at the central zone regressed in size, being replaced by a cuboidal epithelium (Fig. 6d). At the marginal zone, the inner epithelium became columnar, bore long cirri and contained a blue and turquoise-green intracytoplasmic material under the PAS-AB and the trichrome stains, respectively (Fig. 7a–c). An abundant mucinous material was located between both mantle margins, becoming more eosinophilic and deep-blue under the H&E and PAS-AB stains, respectively (Fig. 7a and b).

The digestive tract showed a high differentiation of the different portions with an evident development of cuboidal epithelial cells with cilia (Fig. 7j–m). The oral groove was observed as a broad and ciliated opening with poorly developed labial palps, observed as mild and non-plicated protrusions (Fig. 7j). The oesophagus was plicated and ciliated, surrounded by the cerebroideal ganglion (Fig. 6c and e). The stomach presented a dorsal region with round shape and non-ciliated epithelium covered by a thin gastric shield. At the ventral region, the style sac was funnel-shaped, oriented posteroventrally, lined by a ciliated, pseudostratified columnar epithelium and contained the crystalline style (Fig. 7k–n). Both crystalline style and gastric shield were acellular structures with diffuse limits that stained magenta or light-blue under the PAS-AB and the trichrome stains, respectively (Fig. 7k–n). The lateral region of the stomach is communicated by two openings with the bilobed primordium of the digestive gland (Fig. 6c), which contained refringent, eosinophilic granules of highly variable size up to 6 µm diameter (Fig. 7n). These granules intensely stained PAS positive

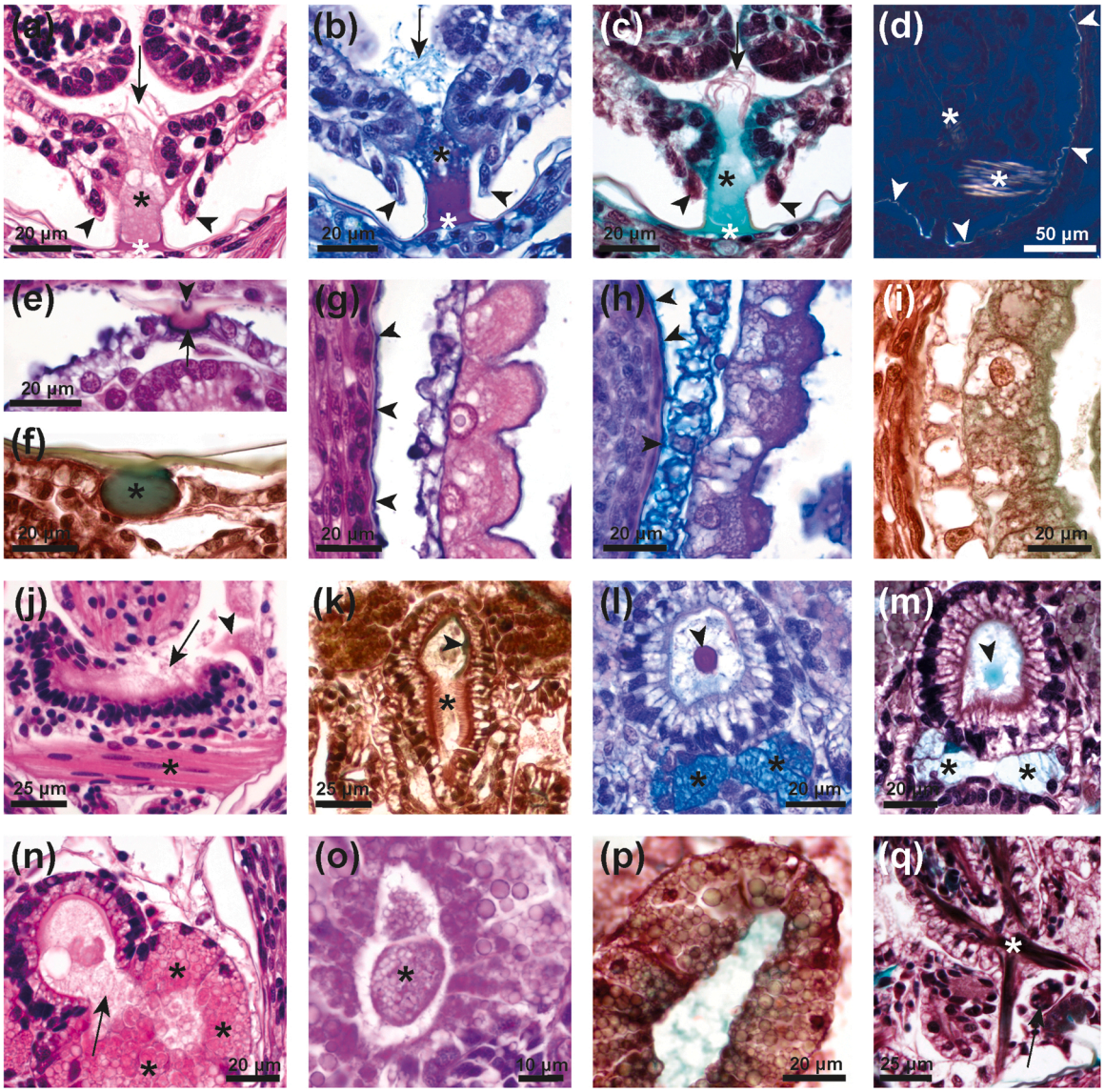

Fig. 7. Stage III of *M. margaritifera* post-larva encysted within the Atlantic salmon gills from the day 200 to the day 220 post-exposure. (a-c) Detail of zip membrane filling the valve cleft (white asterisks), as well as the outer margin (arrowheads) and inner margin of the mantle, the latter provided with long cirri (arrows). Note the lack of continuity of the valve periostracum with the zip membrane and the slightly different staining properties of the zip and the mucinous material located towards the pallial cavity (black asterisks). H&E (a), PAS-AB (b) and trichrome (c) stains. (d) Histological section highlighting the periostracum (arrowheads) and the muscle fibers (asterisks) under polarized light. Trichrome stain. (e) Transversal section of the hinge region showing the fibrous ligament (arrow) underneath the U-shaped ligament (arrowhead). H&E stain. (f) Longitudinal section of the fibrous ligament (asterisk) showing a semioval shape. Trichrome stain. (g-i) Detail of the outer mantle epithelium lying over the periostracum, with a basophilic material in between (arrowheads), stained under the H&E stain (g) and blue under the PAS-AB stain (h), but unstained with the trichrome stain (i). (j) Ciliated simple columnar epithelium of the oral groove (arrow), besides the anterior adductor muscle (asterisk). Note the proximity of one globose mantle cell of the mushroom body (arrowhead). (k) Stomach with the dorsal region covered by a thin gastric shield stained turquoise-green with the trichrome stain (arrowhead), and a funnel-shaped style sac ventrally (asterisk). (l and m) The crystalline style (arrowheads) was visualized magenta and light-blue under the PAS-AB and trichrome stains, respectively. Ventrally to the stomach, the globular gland cells of the byssal complex (asterisks) were observed blue with the PAS-AB stain, but poorly light-blue stained with the trichrome stain. (n) Communication between the stomach and the primordium of the digestive gland (arrow), the latter containing a high number of eosinophilic granules (asterisks). H&E stain. (o and p) Detail of the digestive gland epithelium with abundant PAS-positive and yellowish granules under the PAS and trichrome stain, respectively. Note the vacuolized and finely granular PAS-postive material within the lumen (asterisk, o). (q) Detail of the intestine and rectum (arrow) anatomically related with the muscular chiasma formed by the retractor muscles (asterisk). Trichrome stain.

towards the lumen of the diverticula (Fig. 7o) and were yellowish under the trichrome stain (Fig. 7p). The intestine was lined by ciliated columnar epithelium and formed a short loop inside the visceral mass, but no typhlosole was observed (Figs. 6c and 7q). The rectum passed through the renopericardial region, between the posterior pedal retractor muscles and opened to the pallial cavity at the anal region (Fig. 7q).

Between the paired gill filaments, a ciliated foot extended from the visceral mass towards an antero-ventral position (Fig. 6d and e). It was supported by abundant muscle fibers interposed in multiple directions all over the foot and by two well-developed retractor muscles which created a muscular chiasma dorsally at the medial line (Fig. 7q and Fig. 8a). Two different types of glandular tissue could be observed into the foot, conforming the byssal complex. At the proximal region of the foot, between the pedal ganglia and the stomach, large globular and vacuolized gland cells with PAS positive cytoplasm not stained by H&E

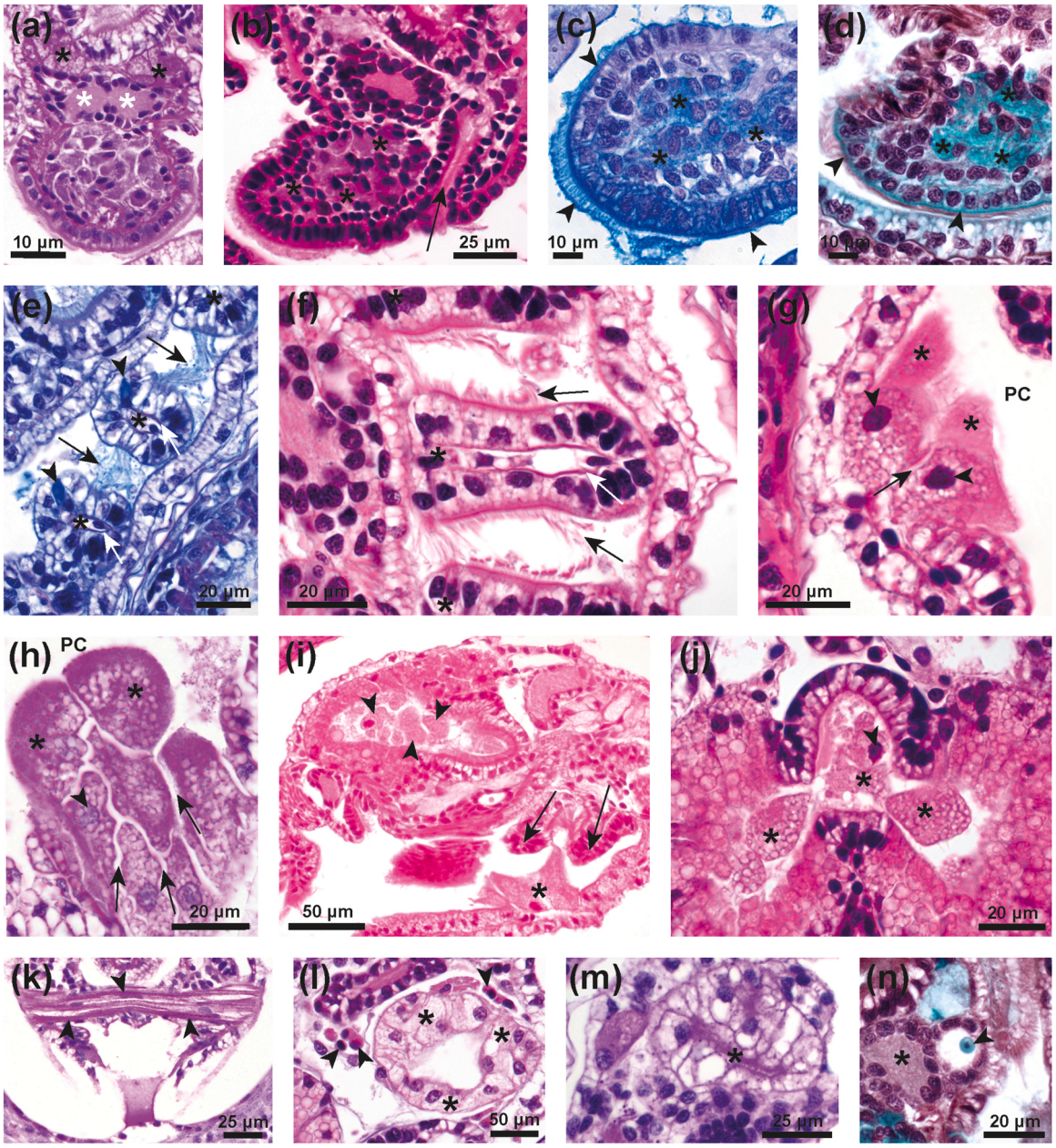

Fig. 8. Stage III of the *M. margaritifera* post-larva encysted within the Atlantic salmon gills between the day 200 and 220 post-exposure. (a) Transversal sections of the foot showing PAS-positive globular gland cells of the byssal complex (black asterisks), in a dorsoposterior location in respect to the bilobed pedal ganglia (white asterisks). PAS stain. (b) Longitudinal section of the foot, exhibiting the byssal duct (arrow) at the posteroventral midline and highly packed subepithelial gland cells of the byssal complex (asterisks) at the apical region. H&E stain. (c and d) Detail of the granular content of the subepithelial gland cells (asterisks) at the apical region of the foot, highlighted blue under the PAS-AB stain and turquoise-green under the trichrome stain. Note the presence of similar staining features at the cytoplasm of the highly ciliated epithelium and over the surface of the foot (arrowheads). (e and f) Three ctenidia (asterisks) positioned between the mantle and the visceral mass, supported by chitinous rods (white arrows) and lined by a ciliated epithelium (black arrows) and a few goblet cells (arrowheads). PAS-AB and H&E stains, respectively. (g and h) Detail of the mushroom body with marked intercellular spaces (arrows), shrunken nucleus (arrowheads) and vacuolized and PAS positive cytoplasmic portions partially sloughed (asterisks) towards the pallial cavity (PC). H&E and PAS stains, respectively. (i) Low magnification showing the remnants of the mushroom body (asterisk) molded by the adjacent ctenidia (arrows) and abundant cellular material (arrowheads) within the lumen of the stomach and the digestive gland primordium. H&E stain. (j) High magnification of the central stomach and the lobulated digestive gland primordium containing cellular fragments with shrunk nucleus (arrowhead) and abundant vacuoles (asterisks). H&E stain. (k) Detail of the posterior adductor muscle conformed by PAS positive myofibers (arrowheads). PAS stain. (l) Renopericardial cavity containing few haemolymphatic cells (arrowheads) and the nephridium with a highly vacuolized epithelium (asterisks). H&E stain. (m) Nephridium displayed an apical cytoplasmic portion with a finely granular PAS positive material oriented towards the lumen (asterisk). PAS stain. (n) Statocyst near the pedal ganglia (asterisk) lined by a cuboidal simple epithelium containing a turquoise-green statolith (arrowhead) with the trichrome stain.

nor the trichrome stain (Fig. 7 m) were observed in a clustered fashion (Fig. 8a). This gland tissue extended towards the posterior region of the foot and opened into a diverticulated and ciliated byssal duct which continued ventrally and opened into the byssal groove, a narrow longitudinal invagination at the posteroventral midline of this organ (Fig. 8b). No byssus thread was observed at the lumen. At the apical region of the foot, a large number or unicellular glands were densely packed underneath the lining epithelium. These gland cells contained

abundant small intracytoplasmic granular material which stained PAS positive and turquoise-green under the trichrome stain; this material was also observed inside the cytoplasm and over the surface of the epithelial cells (Fig. 8a–d). Superficially, the foot was lined by a ciliated, simple columnar epithelium (Fig. 8a–d).

Anchored to the posterior region of the visceral mass, three pairs of ctenidia occupied each lateral region of the pallial cavity (Fig. 8e and f), being oriented towards an antero-ventral direction (Fig. 6d and e). Each ctenidium was highly vascularized, supported by thin chitinous rods and lined by a simple columnar epithelium with few goblet cells (Fig. 8e). The lateral epithelial cells bore abundant long cilia which progressively increased in number during this stage and contacted the cilia of the adjacent filament (Fig. 8 f).

The globose cells which comprised the remaining mushroom body were scarce and presented wide intercellular spaces, a shrunken nucleus and highly vacuolized cytoplasm with abundant PAS positive material at the apical border (Fig. 8g and h). Moreover, abundant cellular portions were observed partially sloughed at the pallial cavity (Fig. 8h) and the

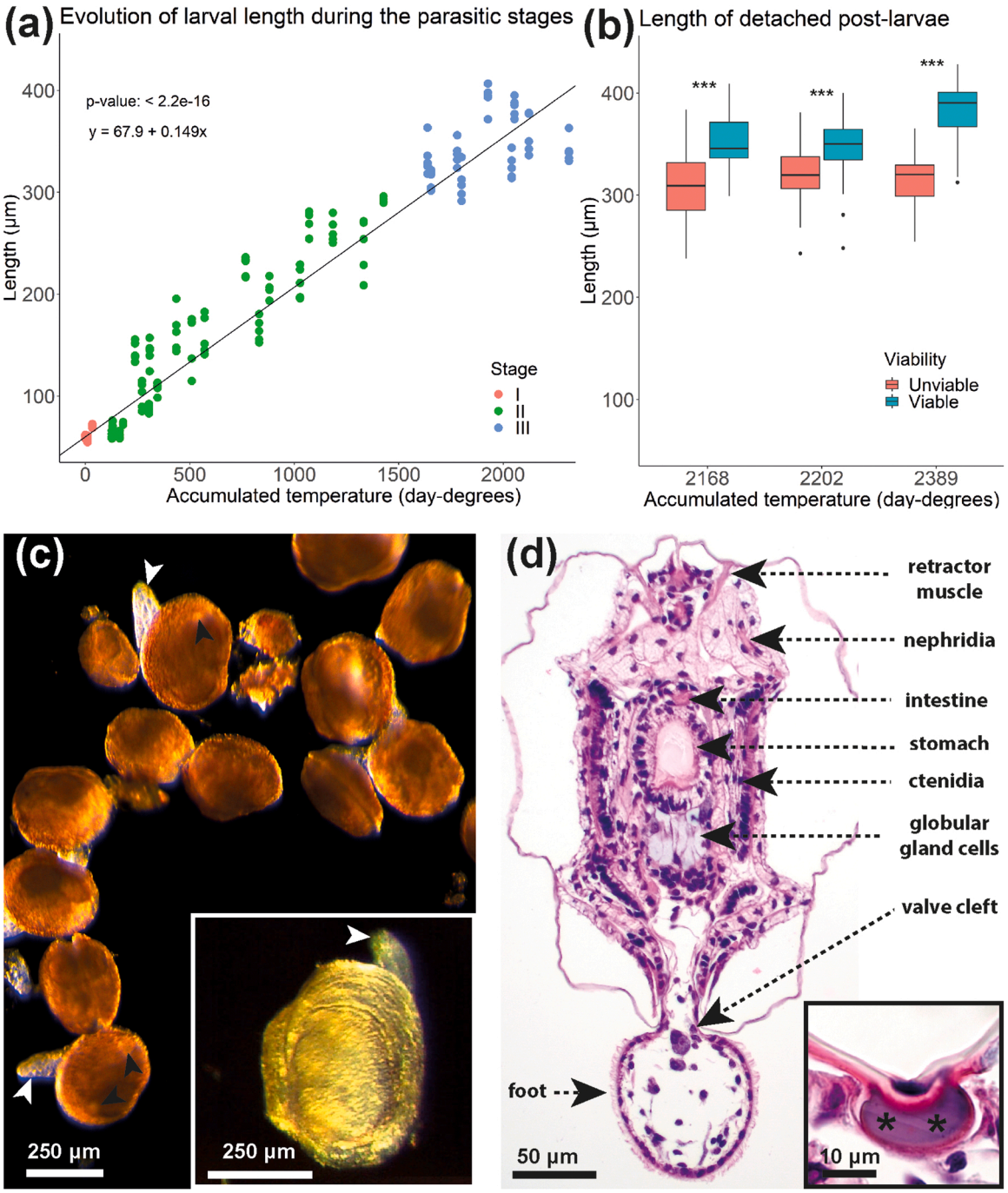

Fig. 9. (a) Evolution of larval length during the three parasitic stages (I-III), highly correlated with the accumulated temperature. (b) The length of the viable detached post-larva showed a significant bigger size than the unviable detached post-larvae (***; *p*-value <0.001). (c) Stereomicrophotograph of the viable post-larva, recently detached from the fish gills with yellowish valves and protruding foot through the valve cleft (white arrowheads). In some specimens, the insertion of both adductor muscles (black arrowheads) could be observed. Inset: details of the external surface of the continuous periostracum without any remnant of the gill tissue. (d) Histological image at low magnification of a detached post-larva, showing a similar morphology to the encysted larvae except for the foot which protruded towards the valve cleft. Inset. Detail of the semioval fibrous ligament at the hinge region (asterisks).

remaining epithelial surface of the cytoplasm displayed concave depressions being molded by the adjacent ciliated ctenidial and pedal epithelia (Fig. 8i). Remnants of cells similar to those aforementioned were observed inside the lumen of the stomach and the primordium of the digestive gland, characterized by a shrunk nucleus, abundant vacuoles and finely PAS positive granular material within the cytoplasm (Figs. 7o, 8i and j).

At the dorsal region, the anterior and posterior adductor muscles measured around 20 μm of diameter and were intermingled by abundant bundles of myofibers (Fig. 8k). The renopericardial cavity was located at the posterodorsal region of the visceral mass, containing a paired and well-developed nephridia, with excretory cells arranged towards a lumen and showing a highly vacuolized cytoplasm with PAS positive substance at the apical border (Fig. 8l and m), and a high number of haemolymphatic cells, as haemolymphatic cells (Fig. 8l). In addition, the complete development of the nervous system was confirmed by the presence of the cerebroideal, visceral and pedal ganglia (Fig. 8a). Besides the bilobed pedal ganglia, a paired statocyst could be identified (Fig. 8 n).

During the three parasitic stages, larvae grew a 670% in length, from 59 ± 2.6 μm to 397 ± 23 μm, and the larval length was positively correlated to the degree-days (Spearman's coefficient.97), displaying a significant linear relationship ($y = 67.9 + 0.149x$, p-value <0.05; Fig. 9a).

After detachment from the gill, the post-larva showed a variable size in which the viable individuals were significantly longer (361 μm) than the unviable ones (314 μm) (p-value <0.001; Fig. 9b). Externally, valves showed ivory, smooth and continuous periostracum lacking any remnant of the previous surrounding gill tissue of the host (Fig. 9c). The internal morphology of the viable post-larva was similar to that described during the previous stage III (Table 1), but lacking the zip membrane, so that the pallial cavity communicated with the medium through the valve cleft, where the foot occasionally protruded towards (Fig. 9d). Dorsally, these valves remained anchored by the semioval fibrous ligament (Inset, Fig. 9d).

4. Discussion

This study provides an exhaustive description of the larval development and organogenesis of the freshwater mussel *M. margaritifera* in the gills of Atlantic salmon (*S. salar*). This knowledge is essential to establish the sequential growth stages of the larva and also to understand the host-parasite interaction, which has been scarcely addressed. Thus, this work aims to illustrate the main morphological changes occurring at this stage and that may help other researchers to interpretate the larval development of naiads. Moreover, this information migh help to optimize the breeding programmes of *M. margaritifera*, where the parasitic stage is an important bottleneck.

During this 7-month parasitism, larvae overwintered in the fish gills and grew over 6-folds in length; up to 308–397 μm, similarly to previous studies in *M. margaritifera* (Araujo et al., 2018; Bauer, 1987; Eybe et al., 2015; Marwaha et al., 2017; Schartum et al., 2016; Young and Williams, 1984). This slow but marked development contrast with other species with larger glochidia with around 200–400 μm length, which showed a negligible growth during its much shorter time encysted into the fish host (Bauer, 1994; Wächtler et al., 2001). Despite this different development rate among species, the organogenesis took place in a similar continuous fashion, divided from two to six sequential stages, as depicted in margaritiferids (Araujo et al., 2002; Scharsack, 1994) and other naiads (Bändel, 1988; Chumnanpuen et al., 2011).

The stage I could be regarded as a short and transitional period in which the typical morphology of the small glochidia vanished. During the first three days of parasitism, the pinched epithelial cells of the gill became rapidly disintegrated (Castrillo et al., 2020), aided by the enzymes contained in the coarse granules of the inner mantle (Lefevre and Curtis, 1912; Pekkarinen and Valovirta, 1996). Subsequently, during the long and intermediate stage II, comprised from the day 14 to the day 150 PE, the encysted larva was enclosed by the valves and the zip membrane in between the valve cleft, providing an interface between the outer gill tissue of the fish and the inner larval tissues.

Valves were articulated at the dorsal region by a U-shaped ligament which might counteract the larval adductor muscle of the glochidia, supporting previous descriptions of the hinge ligament in other naiad described by scanning electron microscopy (Chumnanpuen et al., 2011; Schwartz and Dimock, 2001; Uthaiwan et al., 2001). Once the larval adductor muscle was lost, a fibrous ligament became evident at the terminus of the parasitism and resembled the primitive and provisional ligament structure of *M. margaritifera* which is also vanished six months after detachment from the fish gills (Pennec and Jüngbluth, 1983). These different ligament formations suggest a discontinuous ligament ontogeny as described in several Palaheterodont taxa (Bändel, 1988; Sartori and Ball, 2009).

Each valve was comprised of a single and extremely thin layer of periostracum with no signs of calcification under the alizarin red S stain, similar to previous electron microscopy descriptions of the *M. margaritifera* glochidium (Nezlin et al., 1994; Pekkarinen and Valovirta, 1996). This contrasts with the much thicker shell of many other glochidia within the family Unionidae, which contained an inner and porous calcareous layer underneath the thin periostracum, referred to as cuticle or pellicle (Bändel, 1988; Chumnanpuen et al., 2011; Lasee, 1991; Lima et al., 2006; Rand and Wiles, 1982; Schwartz and Dimock, 2001; Uthaiwan et al., 2001). To structurally support the thin valves of *M. margaritifera* larva, fluid-filled reservoirs described in the flanges could tighten the clasping valves of the glochidia (Pekkarinen and Valovirta, 1996) and, similarly, the fluid enclosed within the encysted larva might also maintain the structure of the larval valves. Nevertheless, the progressive increase in the valve opacity and the accumulation of an acidic material between the periostracum and the outer mantle might indicate the onset of the shell biomineralization towards the end of the parasitic phase (stage III), as has been described during the early shell secretion by the outer mantle epithelium in the post-larval stages of bivalves (Addadi et al., 2006; Checa, 2018).

At the valve cleft, the zip membrane, recently described as a C-shaped proteinaceous barrier located over the valve rims (Castrillo et al., 2020), delimited completely the pallial cavity from the outer gill microenvironment during most of the *M. margaritifera* parasitism. This membrane might isolate the larva and avoid the release of the disintegrated clasped tissue or enzymes from the pallial cavity through the valve cleft, limiting the triggering of the host immune response. However, before the formation of the zip membrane, the material aforementioned is susceptible to elicit an early immune response as described during the first 14 days of glochidiosis, related to the early detachment of immature larva (Castrillo et al., 2020). In this sense, despite a specific immune response against the glochidia of *Lampsilis reeveiana* was described in *Micropterous salmoides*, there is no information about the antigenicity of the parasitic freshwater mussel larvae (Dodd et al., 2006). Further studies need to elucidate the antigenic role of the different larval structures during these critical early stages, which could bet in touch—prior to the formation of the zip membrane—with surrounding gill tissue. Moreover, the external surface of the larva itself, with the scleroproteinaceous periostracum and zip membrane, should not be dismissed.

Considering the extreme thinness of the larval shell, the formation of the zip membrane, and the absence of a functional digestive apparatus during most of the parasitism, non-particulate nutrients of the gill interstitial fluid might diffuse through these external structures and serve as the main source of nutrition to the *M. margaritifera* larva, as evidenced by stable isotope analysis (Denic et al., 2015). This source of nourishment from non-particulate organic matter has been already described in the veliger larva of the family Ostreidae through the velum (Manahan and Crisp, 1982).

In intimate contact with the valves, the mantle of the encysted larva

developed a different morphology than the glochidium, characterized by the extensive mushroom body –a mantle tissue related to the parasitic nutrition from fish which owes its name to its mushroom shape protruding towards the pallial cavity (Blystad, 1923). This organ was described exclusively during the parasitic stage of *M. margaritifera* (Scharsack, 1994) and other few naiads (Arey, 1932; Blystad, 1923; Chumnanpuen et al., 2011). For the first time, the accumulation of lipid droplets during the larval development of *M. margaritifera* was demonstrated by the observation of abundant lipid vacuoles in the larval mantle. These results complement previous descriptions in *Utterbackia imbecillis* larva, in which the mushroom body accumulated lipid droplets and glycogen granules, observed by transmission electron microscopy (Fisher and Dimock, 2002); although no glycogen material was discernible with the PAS-diastase stain in our study. This abundant lipid content could be regarded as energy storage essential for the metamorphosis into post-larva, similar to that described during the early development of marine bivalves (Gallager et al., 1986). Based on the fact that the lipid droplets appeared only while the larva remained encysted in the fish, Fisher and Dimock (2002) hypothesized that the mushroom body might take part in the uptake of nutrients through the microvilli located in their apical surface, in a similar way to the microvillar surface of veliger's velum (Manahan and Crisp, 1982) or the epithelium of the digestive gland of adult bivalves (Owen, 1974). Such microvillar appearance of the mushroom body was also evidenced in *M. margaritifera* by electron microscopy (Scharsack, 1994). Based on this parasitic nutrition, the quantification of the lipid content could serve as a potential indicator of the larval status during the parasitism as described during the development of *Unio crassus* and *Anodonta anatina* juveniles (Douda, 2015). On the other hand, the gill cryosection revealed its potential, not only for the preservation of lipids, but also for the evaluation of the larval structures by reducing the histological fixation artifacts. To deal with the apparition of these artifacts, an thorough selection of the best and most representative images was required.

Due to this morphology and functionality, different from the glochidium, we propose to name "mushroom larva" to the larval form described during the parasitic stage II, grounded in the first descriptions of a similar intermediate "mushroom body stage" coined during the parasitism of naiads (Blystad, 1923). Nevertheless, the marked vacuolization of the mantle of anodontine glochidia, prior to the encystment into the fish (Pekkarinen, 1996; Wood, 1974), may allude to a previous embryonic nourishment during the matrotrophic brooding in those large glochidia with short parasitic periods (Schwartz and Dimock, 2001). Besides nutrition, the larval mantle of naiads has been also proposed as a multifunctional organ involved also in respiratory, osmoregulatory and excretory functions (Castilho et al., 1989; Rand and Wiles, 1982; Schwartz and Dimock, 2001). Some of the most relevant organs involved in the aforementioned functions, i.e., the ctenidia and nephridia, were morphologically absent or non-functional during most of the parasitism; thus, it seems plausible that the extensive larval mantle might counteract the hyperosmotic fish tissue (Nezlin et al., 1994; Pekkarinen and Valovirta, 1996). Further studies are needed to evaluate the permeability of the zip membrane and the periostracum to the nutrients, gases, salts and waste products, together with the potential role that the mantle cells might play in the exchange of these substances as it has been proposed by Robertson and Coney (1979).

From the day 150 to the day 220 PE, the stage III was associated with the larval metamorphosis, characterized histologically by an intense and progressive organogenesis, leading to the detachment of viable post-larva since approximately the day 200 PE (the degree-day 1900–2200 PE), similar to previous studies in which the onset of post-larval detachment started around 1700–1800 day-degrees (Castrillo et al., 2021; Eybe et al., 2015; Marwaha et al., 2017; Taeubert et al., 2013). This detachment was successfully synchronized by the high cumulative temperatures in combination with the increase of water temperature over 15ºC, both considered as important trigger factors of larval metamorphosis (Hruska, 1992; Marwaha et al., 2017; Scheder et al., 2014). On the other hand, it was reported that extremely cold water (1–3ºC) might also slow down this development rate up to a diapause stage (Murzina et al., 2017; Scheder et al., 2014); although this was not observed in this study, since the larval growth was linear (approximately 0.15 μm/day) and temperatures were over 6ºC.

The morphological features described after the day 200 PE –exclusively in the metamorphosed post-larva– could be employed to monitor the larval metamorphosis in the fish gills during the breeding programmes of *M. margaritifera*. Among those features, the indirect observation of the anterior and posterior adductor muscles through the valves might serve as a promising tool to easily distinguish the larval metamorphosis by wet mount of fish gills. This observation is comparable with the formation of the pigmented larva eye spot which precedes the metamorphosis of *Ostrea edulis* (Waller, 1981) or the visualization of the adductor muscles reported in the detached juvenile naiad of *Hyriopsis myersiana* (Kovitvadhi et al., 2007). On the other hand, the presence of globose cells of the mushroom body contrasts with previous studies which described a completely absent mushroom body after 10 months of parasitism (Scharsack, 1994). These mushroom body remnants in the recently detached post-larva might suggest a premature detachment and could be considered as a potential indicator of an incomplete metamorphosis, in which the artificial increase in water temperature might synchronize, but also precipitate the detachment of the outermost larvae (Castrillo et al., 2021).

The appearance of the post-larval organs since the day 200 PE indicated a completely different morphology which is essential for the settlement into the benthos and the acquisition of a deposit-feeding lifestyle, as has been described for the *M. margaritifera* juveniles (Araujo et al., 2018; Lavictoire et al., 2018; Schartum et al., 2016). The post-larva anatomy, acquired at the end of the parasitism, is surprisingly similar to that described during the plantigrade stages in many different species of marine bivalves, which is crucial for the settlement and nourishment in the benthos (Baker and Mann, 1997; Bower and Meyer, 1990; Carriker, 2001).

The post-larval foot was internally characterized by different glandular tissues described for the first time in *M. margaritifera*, resembling some of the glandular tissues which conform the byssal complex of the recently detached juveniles of the freshwater mussel *Lampsilis cardium* (Lasee, 1991) but also other marine bivalves (Gruffydd et al., 1975). The subepithelial gland cells located at the tip of the foot were morphologically similar to the gland type A of *Ostrea edulis* (Cranfield, 1973), which exhibit similarities to the tip attachment glands of scallops *Patinopecten yessoensis* and *Pecten maximus*, where a mucinous merocrine substance is secreted through the epithelium by ducts and is involved in the pedal attachment after metamorphosis (Bower and Meyer, 1990; Gruffydd et al., 1975). Similar cells, termed as "violet cells", were similarly characterized in the foot of other adult freshwater mussels, although the role of these cells has not been elucidated yet (McElwain and Bullard, 2014). In addition to the subepithelial gland cells, globular gland cells extending over the pedal ganglion towards the dorso-posterior region of the foot were morphologically similar to the gland type D4 of *Ostrea edulis* (Cranfield, 1973). Its location and anatomical relation to the byssal duct suggests that this gland tissue corresponded with the primary byssus gland described in scallops (Bower and Meyer, 1990; Gruffydd et al., 1975). This duct opened into the byssal groove, a longitudinal invagination described in the foot of *M. margaritifera* juveniles (Araujo et al., 2018). Nevertheless, the formation of the byssal thread was not confirmed until the formation of a macroscopical byssal thread in more advanced juvenile stages of *M. margaritifera* (Lavictoire et al., 2018), *Lampsilis radiata* and *Elliptio complanata* (Smith, 1998). In absence of a byssal thread after metamorphosis and detachment from the fish gill, the pedal attachment has been proposed in several juvenile naiads as an essential mechanism for the settlement and burrowing by action of the adhesive mucus (Bradley, 2011; French and Ackerman, 2014) and the well-developed muscle system of the foot. Despite the potential role of the byssal complex in the

settlement of juvenile naiads, the post-larval foot remain poorly studied and require further characterization of the different gland tissues and secreted products.

Moreover, these mucinous and/or collagenous secretions observed over the tip of the foot may be involved in the physical and immunitary protection, but also in the agglutination of feeding particles. Considering that deposit-feeding occurs in many autobranch juveniles before the gills are capable of suspension-feeding, the highly protractile and ciliated foot could create a feeding current that transports the fine particulate algae and bacteria from the river sediment to the labial palps (Yeager et al., 1994). Once the food is ingested, the ciliated stomach displayed a similar morphology to the typical type IV stomach of freshwater bivalves, being capable of sorting, triturating and digesting food particles. In communication with the stomach, the bilobed primordium of the digestive gland presented a similar granular appearance to *M. margaritifera* and *P. auricularius* larva at the end of the parasitism (Araujo et al., 2002; Scharsack, 1994), but contrasted with the ductal system of the bivalve's digestive gland, lined by digestive and basophilic cells (Owen, 1974). This different morphology might point towards different post-larval nutrition during and/or rigth after the parasitism, in which the abundant granules might correspond with a proteinaceous material involved in the enzymatic digestion and extracellular digestion of the digestive gland.

Within the lumen of the stomach and digestive gland primordium, a large number of vacuolized cell fragments were present, similarly to that described at the end of the parasitic stage in other freshwater mussels (Arey, 1932; Chumnanpuen et al., 2011; Scharsack, 1994) and resembled sloughed cell fragments from the mushroom body to the pallial cavity. This abundant material inside the digestive lumen when the valves remained closed by the zip membrane leads to the speculation that the mushroom body might be detached and ingested, similar to the ingestion of the large test cells during the metamorphosis of the primitive encapsulated pericalymma larva of protobranch bivalves (Okusu, 2002; Zardus and Morse, 1998). To support this hypothesis, further studies are needed to corroborate this ingestion and reuse of the mushroom body and discard other potential physiological processes of the digestive gland related to the rhythmic feeding of bivalves (Owen, 1974).

The observation of the ctenidia during the stage III of *M. margaritifera* development provides the first histological evidence of the early gill formation during metamorphosis of this species, being complementary of the previous scanning electron microscopy description by Scharsack (1994). The presence of gill filaments, endowed with lateral cilia and the haemolymphatic vessels underneath, suggests that gills were able to generate a ciliary water current and haemolymphatic circulation, essential for respiration. On the other hand, the unreflected and partially ciliated ctenidia, only located at the inner demibranch, resemble the first post-larval stages which are not completely effective for suspension-feeding until the first year post-detachment (Lavictoire et al., 2018; Schartum et al., 2016).

Based on the continuous larval development of *M. margaritifera* described in three parasitic stages (I–III), the morphogenesis from glochidia to post-larva was observed, highlighting an intermediate larval stage with unique morphological features involved in the parasitic interaction between the bivalve larva and the fish host. In conclusion, this study provides an overview of the larval morphogenesis of *M. margaritifera*, from glochidium to post-larva, essential for understanding the parasitic interaction between the freshwater mussel larva and the fish host. The intermediate stage—termed as "mushroom larva"—was characterized by a distinct morphology among bivalves in which the mushroom body and the zip membrane might be involved in both isolation and nutrition from the host fish. After metamorphosis and detachment from the gills, these unique larval structures are lost and the complete set of post-larval organs and structures allowed to continue with their free-living stage in the riverbed. Simultaneously, the morphological techniques and the hallmarks described in this sequential larval development (i.e., the lipid content and the presence of the adductor muscle at metamorphosis) could be directly employed to optimize and monitor the larval developmental status during the most critical stages within the conservation programmes of this endangered bivalve. In addition, the techniques developed in this study are susceptible of being employed in further studies to better understand the role of these larval and juvenile anatomical structures, focusing on the glochidium encystment, development of the mushroom larvae, and metamorphosis into juvenile mussels.

Declaration of Competing Interest

The authors declare the following financial interests/personal relationships which may be considered as potential competing interests: Paz Ondina reports financial support was provided by Fundación Biodiversidad (Ministerio para la Transición Ecológica y el Reto Demográfico). Pedro A. Castrillo reports financial support was provided by Ministerio de Educación, Cultura y Deporte. Paz Ondina reports financial support and equipment, drugs, or supplies were provided by Dirección Xeral de Patrimonio Natural, Consellería de Medio Ambiente, Territorio e Vivenda (Xunta de Galicia).

Data Availability

Data will be made available on request.

Acknowledgements

The authors would like to thank the assistance of Dr. R. Mascato and R. Ocharan with the fieldwork and the husbandry procedures during this long-term experimental trial. Also, we warmly thank S. Maceiras for the thorough histopathological technical assistance. We also want to thank Dr. Antonio Villaba and Rafael Araujo for their comments during the interpretation and discussion of the results. This study was supported by the European Project Life Margal Ulla, Fundación Biodiversidad (Ministerio para la Transición Ecológica y el Reto Demográfico) and Dirección Xeral de Patrimonio Natural, Consellería de Medio Ambiente, Territorio e Vivenda (Xunta de Galicia). P. A. Castrillo held a University Professorship Formation (FPU) grant from the Ministerio de Educación, Cultura y Deporte.

References

Addadi, L., Joester, D., Nudelman, F., Weiner, S., 2006. Mollusk shell formation: a source of new concepts for understanding biomineralization processes. Chem. A Eur. J. 12 (4), 980–987. https://doi.org/10.1002/chem.200500980.

AnonR Core Team. 2019). R: a language and environment for statistical computing: R Foundation for Statistical Computing, Vienna, Austria. Retrieved from ⟨https://www.R-project.org/⟩.

Araujo, R., Camara, N., Ramos, M.A., 2002. Glochidium metamorphosis in the endangered freshwater mussel *Margaritifera auricularia* (Spengler, 1793): a histological and scanning electron microscopy study. J. Morphol. 254 (3), 259–265. https://doi.org/10.1002/jmor.10031.

Araujo, R., Campos, M., Feo, C., Varela, C., Soler, J., Ondina, P., 2018. Who wins in the weaning process? Juvenile feeding morphology of two freshwater mussel species. J. Morphol. 279 (1), 4–16. https://doi.org/10.1002/jmor.20748.

Arey, L.B., 1932. The nutrition of glochidia during metamorphosis. A microscopical study of the sources and manner of utilization of the nutritive substances. J. Morphol. 53 (1), 201–221. https://doi.org/10.1002/jmor.1050530108.

Baker, P., Mann, R., 1997. The postlarval phase of bivalve mollusks: a review of functional ecology and new records of postlarval drifting of Chesapeake Bay bivalves. Bull. Mar. Sci. 61, 409–430.

Bändel, K., 1988. Stages in the ontogeny and a model of the evolution of bivalves (Mollusca. Paläontol. Z. 62 (3), 217–254. https://doi.org/10.1007/BF02989494.

Barnhart, M.C., Haag, W.R., Roston, W.N., 2008. Adaptations to host infection and larval parasitism in Unionoida. J. North Am. Benthol. Soc. 27 (2), 370–394. https://doi.org/10.1899/07-093.1.

Bauer, G., 1987. The parasitic stage of the freshwater pearl mussel. II. Suspect brown trout. Arch. fur Hydrobiol. 76, 403–412.

Bauer, G., 1994. The adaptive value of offspring size among freshwater mussels (Bivalvia; Unionoidea. J. Anim. Ecol. 63 (4), 933–944. https://doi.org/10.2307/5270.

Blystad, C.N., 1923. Significance of larval mantle of fresh-water mussels during parasitism, with notes on a new mantle condition exhibited by *Lampsilis luteola*. Bull. Bur. Fish. *39*.

Boeker, C., Lueders, T., Mueller, M., Pander, J., Geist, J., 2016. Alteration of physico-chemical and microbial properties in freshwater substrates by burrowing invertebrates. Limnologica 59, 131–139. https://doi.org/10.1016/j.limno.2016.05.007.

Bower, S.M., Meyer, G.R., 1990. Atlas of anatomy and histology of larvae and early juvenile stages of Japanese scallop (*Patinopecten yessoensis*). Can. Spec. Publ. Fish. Aquat. Sci. 111, 51.

Bradley, M.E., 2011). Byssus production in freshwater mussels (Bivalvia: Unionoidea). (Master of Science, Biology Doctoral dissertation), Missouri State University, Springfield. MSU Graduate Theses (11295) database. ⟨https://bearworks.missouristate.edu/theses/1295/⟩.

Carriker, M.R., 2001. Chapter 3 Embryogenesis and organogenesis of veligers and early juveniles. In: Kraeuter, J.N., Castagna, M. (Eds.), Developments in Aquaculture and Fisheries Science, Vol. 31. Elsevier, pp. 77–115.

Castilho, F., Machado, J., Reis, M.L., Sá, C., 1989. Ultrastructural study of the embryonic and larval shell of *Anodonta cygnea*. Can. J. Zool. 67 (7), 1659–1664. https://doi.org/10.1139/z89-238.

Castrillo, P.A., Varela-Dopico, C., Ondina, P., Quiroga, M.I., Bermúdez, R., 2020. Early stages of *Margaritifera margaritifera* glochidiosis in Atlantic salmon: morphopathological characterization. J. Fish. Dis. 43 (1), 69–80. https://doi.org/10.1111/jfd.13100.

Castrillo, P.A., Varela-Dopico, C., Bermúdez, R., Ondina, P., Quiroga, M.I., 2021. Morphopathology and gill recovery of Atlantic salmon during the parasitic detachment of *Margaritifera margaritifera*. J. Fish. Dis. 44 (8), 1101–1115. https://doi.org/10.1111/jfd.13372.

Checa, A.G., 2018. Physical and biological determinants of the fabrication of molluscan shell microstructures. Front. Mar. Sci. 5 (353) https://doi.org/10.3389/fmars.2018.00353.

Chumnanpuen, P., Kovitvadhi, U., Chatchavalvanich, K., Thongpan, A., Kovitvadhi, S., 2011. Morphological development of glochidia in artificial media through early juvenile of freshwater pearl mussel, *Hyriopsis* (*Hyriopsis*) *bialatus* Simpson, 1900. Invertebr. Reprod. Dev. 55 (1), 40–52. https://doi.org/10.1080/07924259.2010.548643.

Cranfield, H.J., 1973. Observations on the function of the glands of the foot of the pediveliger of *Ostrea edulis* during settlement. Mar. Biol. 22 (3), 211–223. https://doi.org/10.1007/BF00389175.

Denic, M., Taeubert, J.E., Geist, J., 2015. Trophic relationships between the larvae of two freshwater mussels and their fish hosts. Invertebr. Biol. 134 (2), 129–135. https://doi.org/10.1111/ivb.12080.

Dodd, B.J., Barnhart, M.C., Rogers-Lowery, C.L., Fobian, T.B., Dimock, R.V., 2006. Persistence of host response against glochidia larvae in *Micropterus salmoides*. Fish. Shellfish Immunol. 21 (5), 473–484. https://doi.org/10.1016/j.fsi.2006.02.002.

Douda, K., 2015. Host-dependent vitality of juvenile freshwater mussels: implications for breeding programs and host evaluation. Aquaculture 445, 5–10. https://doi.org/10.1016/j.aquaculture.2015.04.008.

Eybe, T., Thielen, F., Bohn, T., Sures, B., 2015. Influence of the excystment time on the breeding success of juvenile freshwater pearl mussels (*Margaritifera margaritifera*). Aquat. Conserv.: Mar. Freshw. Ecosyst. 25 (1), 21–30. https://doi.org/10.1002/aqc.2471.

Fisher, G.R., Dimock, R.V., 2002. Ultrastructure of the mushroom body: digestion during metamorphosis of *Utterbackia imbecillis* (Bivalvia: Unionidae). Invertebr. Biol. 121 (2), 126–135. https://doi.org/10.1111/j.1744-7410.2002.tb00053.x.

French, S.K., Ackerman, J.D., 2014. Responses of newly settled juvenile mussels to bed shear stress: implications for dispersal. Freshw. Sci. 33 (1), 46–55. https://doi.org/10.1086/674983.

Gallager, S.M., Mann, R., Sasaki, G.C., 1986. Lipid as an index of growth and viability in three species of bivalve larvae. Aquaculture 56 (2), 81–103. https://doi.org/10.1016/0044-8486(86)90020-7.

Geist, J., Auerswald, K., 2007. Physicochemical stream bed characteristics and recruitment of the freshwater pearl mussel (*Margaritifera margaritifera*). Freshw. Biol. 52 (12), 2299–2316. https://doi.org/10.1111/j.1365-2427.2007.01812.x.

Gruffydd, L.D., Lane, D.J.W., Beaumont, A.R., 1975. The glands of the larval foot in *Pecten maximus* L. and possible homologues in other bivalves. J. Mar. Biol. Assoc. U. Kingd. 55 (2), 463–476. https://doi.org/10.1017/S0025315400016064.

Gum, B., Lange, M., Geist, J., 2011.). A critical reflection on the success of rearing and culturing juvenile freshwater mussels with a focus on the endangered freshwater pearl mussel (*Margaritifera margaritifera* L.). Aquat. Conserv.: Mar. Freshw. Ecosyst. 21 (7), 743–751. https://doi.org/10.1002/aqc.1222.

Howard, A.D., Anson, B., 1922. Phases in the parasitism of the unionidae. J. Parasitol. 9, 68.

Hruska, J., 1992. The freshwater pearl mussel in South Bohemia: evaluation of the effect of temperature on reproduction, growth and age structure of the population. Arch. Fur Hydrobiol. 126 (2), 181–191.

Kat, P.W., 1984. Parasitism and the Unionacea (Bivalvia. Biol. Rev. 59 (2), 189–207. https://doi.org/10.1111/j.1469-185X.1984.tb00407.x.

Kovitvadhi, S., Kovitvadhi, U., Sawangwong, P., Machado, J., 2007. Morphological development of the juvenile through to the adult in the freshwater pearl mussel, *Hyriopsis* (Limnoscapha) *myersiana*, under artificial culture. Invertebr. Reprod. Dev. 50 (4), 207–218. https://doi.org/10.1080/07924259.2007.9652248.

Lasee, B.A., 1991. Histological and ultrastructural studies of larval and juvenile Lampsilis (Bivalvia) from the upper Mississippi River. (Doctor of Philosophy Doctoral dissertation), Iowa State University. Iowa State University Digital Repository (10653) database,, Ames, Iowa.

Lavictoire, L., Ramsey, A.D., Moorkens, E.A., Souch, G., Barnhart, M.C., 2018. Ontogeny of juvenile freshwater pearl mussels, *Margaritifera margaritifera* (Bivalvia: Margaritiferidae). PLoS ONE 13 (3), e0193637. https://doi.org/10.1371/journal.pone.0193637.

Lima, P., Kovitvadhi, U., Kovitvadhi, S., Machado, J., 2006. In vitro culture of glochidia from the freshwater mussel *Anodonta cygnea*. Invertebr. Biol. 125 (1), 34–44. https://doi.org/10.1111/j.1744-7410.2006.00037.x.

Lopes-Lima, M., Froufe, E., Do, V.T., Ghamizi, M., Mock, K.E., Kebapçı, Ü., Klishko, O., Kovitvadhi, S., Kovitvadhi, U., Paulo, O.S., Pfeiffer, J.M., Raley, M., Riccardi, N., Şereflişan, H., Sousa, R., Teixeira, A., Varandas, S., Wu, X., Zanatta, D.T., Zieritz, A., Bogan, A.E., 2017a. Phylogeny of the most species-rich freshwater bivalve family (Bivalvia: Unionida: Unionidae): defining modern subfamilies and tribes. Mol. Phylogenetics Evol. 106, 174–191. https://doi.org/10.1016/j.ympev.2016.08.021.

Lopes-Lima, M., Sousa, R., Geist, J., Aldridge, D.C., Araujo, R., Bergengren, J., Bespalaya, Y., Bódis, E., Burlakova, L., Van Damme, D., Douda, K., Froufe, E., Georgiev, D., Gumpinger, C., Karatayev, A., Kebapçi, Ü., Killeen, I., Lajtner, J., Larsen, B.M., Lauceri, R., Legakis, A., Lois, S., Lundberg, S., Moorkens, E., Motte, G., Nagel, K.-O., Ondina, P., Outeiro, A., Paunovic, M., Prié, V., von Proschwitz, T., Riccardi, N., Rudzīte, M., Rudzītis, M., Scheder, C., Seddon, M., Şereflişan, H., Simić, V., Sokolova, S., Stoeckl, K., Taskinen, J., Teixeira, A., Thielen, F., Trichkova, T., Varandas, S., Vicentini, H., Zajac, K., Zajac, T., Zogaris, S., 2017b. Conservation status of freshwater mussels in Europe: state of the art and future challenges. Biol. Rev. 92 (1), 572–607. https://doi.org/10.1111/brv.12244.

Lopes-Lima, M., Bolotov, I.N., Do, V.T., Aldridge, D.C., Fonseca, M.M., Gan, H.M., Gofarov, M.Y., Kondakov, A.V., Prié, V., Sousa, R., Varandas, S., Vikhrev, I.V., Teixeira, A., Wu, R.-W., Wu, X., Zieritz, A., Froufe, E., Bogan, A.E., 2018. Expansion and systematics redefinition of the most threatened freshwater mussel family, the Margaritiferidae. Mol. Phylogenetics Evol. 127, 98–118. https://doi.org/10.1016/j.ympev.2018.04.041.

Manahan, D.T., Crisp, D.J., 1982. The role of dissolved organic material in the nutrition of pelagic larvae: amino acid uptake by bivalve veligers. Am. Zool. 22 (3), 635–646. https://doi.org/10.1093/icb/22.3.635.

Marwaha, J., Jensen, K.H., Jakobsen, P.J., Geist, J., 2017. Duration of the parasitic phase determines subsequent performance in juvenile freshwater pearl mussels (*Margaritifera margaritifera*). Ecol. Evol. 7 (5), 1375–1383. https://doi.org/10.1002/ece3.2740.

McElwain, A., Bullard, S.A., 2014. Histological atlas of freshwater mussels (Bivalvia, Unionidae): *Villosa nebulosa* (Ambleminae: Lampsilini), *Fusconaia cerina* (Ambleminae: Pleurobemini) and *Strophitus connasauganensis* (Unioninae: Anodontini). Malacologia 57 (1), 99–239. https://doi.org/10.4002/040.057.0104.

Murzina, S.A., Ieshko, E.P., Zotin, A.A., 2017. The freshwater pearl mussel *Margaritifera margaritifera* L.: metamorphosis, growth, and development dynamics of encysted glochidia. Biol. Bull. 44 (1), 6–13. https://doi.org/10.1134/s106235901701006x.

Nezlin, L.P., Cunjak, R.A., Zotin, A.A., Ziuganov, V.V., 1994. Glochidium morphology of the freshwater pearl mussel (*Margaritifera margaritifera*) and glochidiosis of Atlantic salmon (*Salmo salar*): a study by scanning electron microscopy. Can. J. Zool. -Rev. Can. De. Zool. 72 (1), 15–21. https://doi.org/10.1139/z94-003.

Okusu, A., 2002. Embryogenesis and development of epimenia babai (Mollusca Neomeniomorpha). Biol. Bull. 203 (1), 87–103. https://doi.org/10.2307/1543461.

Owen, G., 1974. Feeding and digestion in the bivalvia. Adv. Comp. Physiol. Biochem. 5 (0), 1–35. https://doi.org/10.1016/b978-0-12-011505-1.50007-4.

Pekkarinen, M., 1996. Scanning electron microscopy, whole-mount histology, and histochemistry of two anodontine glochidia (Bivalvia: Unionidae. Can. J. Zool. 74 (11), 1964–1973. https://doi.org/10.1139/z96-223.

Pekkarinen, M., Valovirta, I., 1996.). Anatomy of the glochidia of the freshwater pearl mussel, *Margaritifera margaritifera* (L.). Arch. fur Hydrobiol. 137 (3), 411–423. https://doi.org/10.1127/archiv-hydrobiol/137/1996/411.

Pennec, M.L., Jüngbluth, J.H., 1983. The ligamental formations of *Margaritifera margaritifera* (L.) (Bivalvia: Margaritiferidae) and *Mytilus edulis* (L.) (Bivalvia: Mytilidae) during larval and postlarval ontogenesis. J. Mar. Biol. Assoc. U. Kingd. 63 (2), 289–294. https://doi.org/10.1017/S0025315400070673.

Rand, T.G., Wiles, M., 1982. Species differentiation of the glochidia of *Anodonta cataracta* Say, 1817 and *Anodonta implicata* Say, 1829 (Mollusca: Unionidae) by scanning electron microscopy. Can. J. Zool. 60 (7), 1722–1727. https://doi.org/10.1139/z82-224.

Robertson, J.L., Coney, C.C., 1979. Punctal canals in the shell of *Musculium securis* (Bivalvia: Pisidiidae). Malacol. Rev. 12, 37–40.

Rueden, C.T., Schindelin, J., Hiner, M.C., DeZonia, B.E., Walter, A.E., Arena, E.T., Eliceiri, K.W., 2017. ImageJ2: ImageJ for the next generation of scientific image data. BMC Bioinforma. 18 (1), 529. https://doi.org/10.1186/s12859-017-1934-z.

Sartori, A.F., Ball, A.D., 2009. Morphology and postlarval development of the ligament of *Thracia phaseolina* (Bivalvia: Thraciidae), with a discussion of model choice in allometric studies. J. Mollusca Stud. 75 (3), 295–304. https://doi.org/10.1093/mollus/eyp029.

Scharsack, G., 1994. Licht- und elektronenmikroskopische Untersuchungen an Larvalstadien einheimischer Unionacea (Bivalvia; Eulamellibranchiata) [Light and electron microscopic studies on larval stages of native Unionacea (Bivalvia, Eulamellibranchiata)]. (Doctoral dissertation), Universität Hannover, Hannover, Germany. Leibniz Universität Hannover database,.

Schartum, E., Mortensen, S., Pittman, K., Jakobsen, P.J., 2016. From pedal to filter feeding: ctenidial organogenesis and implications for feeding in the postlarval freshwater pearl mussel *Margaritifera margaritifera* (Linnaeus, 1758). J. Mollusca Stud. 83 (1), 36–42. https://doi.org/10.1093/mollus/eyw037.

Scheder, C., Gumpinger, C., Csar, D., 2011. Application of a fivestage field key for the larval development of the freshwater pearl mussel (*Margaritifera margaritifera* L., 1758) under different temperature conditions. In: Thielen, F. (Ed.), Rearing of

unionoid mussels (with special emphasis on the Freshwater Pearl Mussel Margaritifera margaritifera). Ferrantia 64. Musée national d'histoire naturelle, Luxembourg, Luxembourg, pp. 13–22.
Scheder, C., Lerchegger, B., Jung, M., Csar, D., Gumpinger, C., 2014. Practical experience in the rearing of freshwater pearl mussels (*Margaritifera margaritifera*): advantages of a work-saving infection approach, survival, and growth of early life stages. Hydrobiologia 735 (1), 203–212. https://doi.org/10.1007/s10750-013-1516-7.
Schwartz, M.L., Dimock, R.V., 2001. Ultrastructural evidence for nutritional exchange between brooding unionid mussels and their glochidia larvae. Invertebr. Biol. 120 (3), 227–236. https://doi.org/10.1111/j.1744-7410.2001.tb00033.x.
Smith, D.G., 1998). Investigations of the byssal gland in juvenile unionids. Paper presented at the Proceedings of the Conservation, Captive Care, and Propagation of Freshwater Mussel Symposium. ⟨https://molluskconservation.org/FMCS/Workshops/1998–9/Symp1998–1999Proc.html⟩.
Strayer, D.L., 2017. What are freshwater mussels worth? Freshw. Mollusk Biol. Conserv. 20 (2), 103–113, 111.
Taeubert, J.E., Gum, B., Geist, J., 2013. Variable development and excystment of freshwater pearl mussel (*Margaritifera margaritifera* L.) at constant temperature. Limnol. - Ecol. Manag. Inland Waters 43 (4), 319–322. https://doi.org/10.1016/j.limno.2013.01.002.
Uthaiwan, K., Chatchavalvanich, K., Noparatnaraporn, N., Machado, J., 2001. Scanning electron microscopy of glochidia and juveniles of the freshwater mussel, *Hyriopsis myersiana*. Invertebr. Reprod. Dev. 40 (2–3), 143–151. https://doi.org/10.1080/07924259.2001.9652714.
Vaughn, C.C., 2018. Ecosystem services provided by freshwater mussels. Hydrobiologia 810 (1), 15–27. https://doi.org/10.1007/s10750-017-3139-x.
Vaughn, C.C., Hakenkamp, C.C., 2001. The functional role of burrowing bivalves in freshwater ecosystems. Freshw. Biol. 46 (11), 1431–1446. https://doi.org/10.1046/j.1365-2427.2001.00771.x.
Vaughn, C.C., Nichols, S.J., Spooner, D.E., 2008. Community and foodweb ecology of freshwater mussels. J. North Am. Benthol. Soc. 27 (2), 409–423. https://doi.org/10.1899/07-058.1.
Wächtler, K., Dreher-Mansur, M., Richter, T., 2001. Larval types and early postlarval biology in naiads (Unionoida). In: Bauer, G., Wächtler, K. (Eds.), Ecology and Evolution of the Freshwater Mussels Unionoida, Vol. 145. Springer Berlin Heidelberg, pp. 93–125.
Waller, T.R., 1981. Functional morphology and development of veliger larvae of the European oyster, Ostrea edulis Linné. Smithsonian Institution Press,, Washington.
Wood, E.M., 1974. Development and morphology of the glochidium larva of *Anodonta cygnea* (Mollusca: Bivalvia). J. Zool. 173 (1), 1–13. https://doi.org/10.1111/j.1469-7998.1974.tb01743.x.
Yeager, M.M., Cherry, D.S., Neves, R.J., 1994. Feeding and burrowing behaviors of juvenile rainbow mussels, *Villosa iris* (Bivalvia:Unionidae). J. North Am. Benthol. Soc. 13 (2), 217–222. https://doi.org/10.2307/1467240.
Young, M., Williams, J., 1984. The reproductive biology of the freshwater pearl mussel *Margaritifera margaritifera* (Linn.) in Scotland. II. Laboratory studies. Arch. fur Hydrobiol. 100, 29–43.
Zardus, J.D., Morse, M.P., 1998. Embryogenesis, morphology and ultrastructure of the pericalymma Larva of *Acila castrensis* (bivalvia: protobranchia: nuculoida). Invertebr. Biol. 117 (3), 221–244. https://doi.org/10.2307/3226988.